The Photochemistry and Electronic Structures of Metal Carbonyl Cluster Complexes

Thesis by

David R. Tyler

In Partial Fulfillment of the Requirements

for the Degree of

Doctor of Philosophy

California Institute of Technology

Pasadena, California

1979

(Submitted April 6, 1979)

Acknowledgments

Thanks to David Dooley for help with the MCD and EPR spectra,to Bob Gagne for loaning me the small glove box, and to David Erwin for the mass spectra and gas measurements.

The entire Gray Group is recognized for their many contributions to this thesis. Penny Schlusser, Nate Lewis, and Mr. West are singled out for particularly frank and friendly discussions.

A special thanks goes to David Dooley, Kent Mann, and especially Bill Trogler for patiently teaching me new techniques and for showing me how the Big Boys do chemistry.

Of course, Harry is acknowledged for support and for showing me how the Biggest Boys do chemistry.

Maryke Schmidt and Mark Altobelli are thanked for their substantial contributions to this thesis.

Finally and most of all, I thank Kim for the one million sacrifices she made because she was married to a graduate student. This thesis is dedicated to her and to the Littlest Buckaroo.

ABSTRACT

The electronic structures and spectra of the $M_3(CO)_{12}$ (M = Fe, Ru, Os) complexes are discussed. Using techniques such as single crystal polarized spectroscopy and MCD spectroscopy it is shown that the two lowest energy electronic transitions in these complexes are the $\sigma \rightarrow \sigma^*$ (xz (bonding) $\rightarrow$ xz (antibonding)) and $\sigma^{*\prime} \rightarrow \sigma^*$ (z^2 (antibonding) $\rightarrow$ xz (antibonding)) transitions.

Photolysis of $Ru_3(CO)_{12}$ leads to fragmentation of the cluster complex; however, a photochemical study of $Os_3(CO)_{12}$ showed that Os - CO dissociation is a more efficient photoprocess than Os - Os bond cleavage. The different photochemical behaviors of the two cluster complexes is ascribed to their different lowest excited states. The lowest excited state of $Ru_3(CO)_{12}$ is $\sigma \rightarrow \sigma^*$, a state which certainly leads to metal-metal bond cleavage. The $\sigma^{*\prime} \rightarrow \sigma^*$ state is lowest in $Os_3(CO)_{12}$. Electronic excitation to this state does not lead to efficient cluster fragmentation.

The effects of bridging ligands on photochemical metal-metal bond cleavage were also studied. It was found that the bridging CO groups prevent photofragmentation of the $(h^5\text{-}C_5H_5)_2Fe_2(CO)_4$ molecule and also of the $Fe_3(CO)_{11}^{2-}$ complex. In the latter molecule, Fe-CO dissociation is the primary photoprocess. In the case of $(h^5\text{-}C_5H_5)_2Fe_2(CO)_4$, the primary photoproduct is a CO-bridged dimer which has no metal-metal bond.

TABLE OF CONTENTS

CHAPTER 1

Electronic Structures and Spectra of Trinuclear Carbonyl Complexes

David R. Tyler, Robert A. Levenson, and Harry B. Gray

Contribution No. 5789 from the Arthur Amos Noyes Laboratory of Chemical Physics, California Institute of Technology, Pasadena, California 91125

Abstract: Detailed experimental studies of the electronic spectra of trinuclear metal carbonyls have been made. An extended Hückel molecular orbital calculation on D_{3h} $Ru_3(CO)_{12}$ has been performed to aid in assigning the spectra of the triangular cluster complexes. A band at 390 nm (2.56 μm^{-1}) in the spectrum of $Ru_3(CO)_{12}$ is polarized in the plane of the Ru_3 triangle, exhibits an MCD A term, and blue shifts and sharpens on cooling to 77° K. This band is assigned to the $^1A_1' \rightarrow {}^1E'$(xz (bonding) → xz (antibonding)), or $\sigma \rightarrow \sigma^*$ transition. A weak band at 320 nm (3.12 μm^{-1}) is assigned to the $^1A_1' \rightarrow {}^1E'$ (z^2 (antibonding) → xz (antibonding)), or $\sigma^{*\prime} \rightarrow \sigma^*$ transition. Similar evidence suggests that bands at 330 nm (3.03 μm^{-1}) and 385 nm (2.60 μm^{-1}) in the spectrum of $Os_3(CO)_{12}$ be assigned to $\sigma \rightarrow \sigma^*$ and $\sigma^{*\prime} \rightarrow \sigma^*$ transitions, respectively. The relative energies of the $\sigma \rightarrow \sigma^*$ and $\sigma^{*\prime} \rightarrow \sigma^*$ transitions in the $M_3(CO)_{12}$, $Ru_3(CO)_9(PR_3)_3$, and $Fe_nRu_{3-n}(CO)_{12}$ (n = 0-3) molecules depend on the ligand field splitting of the xz and z^2 orbitals in the corresponding $M(CO)_4$ and $Ru(CO)_3PR_3$ fragments. A single crystal polarized spectrum of $Fe_3(CO)_{12}$ shows that the two lowest energy bands at 602 and 437 nm (1.66 and 2.29 μm^{-1}) are polarized in the plane of the Fe_3 triangle. These bands are assigned to the $\sigma^{*\prime} \rightarrow \sigma^*$ and $\sigma \rightarrow \sigma^*$ transitions, respectively. Intense bands ($\varepsilon_M > 25{,}000$) at approximately 4.0 μm^{-1} are assigned to MLCT transitions in the $M_3(CO)_{12}$ molecules. An MO scheme for the D_{4h} molecules $M_2Fe(CO)_{14}$ (M = Mn, Re) is presented. The lowest energy

allowed transition in each of these molecules is predicted to be of the metal-metal σ to σ^* type ($^1A_{1g} \rightarrow {}^1A_{2u}(a_{2u} \rightarrow 2a_{1g})$). The lowest energy band in the spectrum of $Re_2Fe(CO)_{14}$ (2.63 μm^{-1}) is polarized along the ReFeRe axis, consistent with the $^1A_{1g} \rightarrow {}^1A_{2u}$ assignment.

Previous work on the electronic spectra of dimanganese decacarbonyl and related species has shown that the lowest energy absorption bands are attributable to $\sigma \rightarrow \sigma^*$ and $d\pi \rightarrow \sigma^*$ transitions, with the σ and σ^* orbitals being the bonding and antibonding metal $d\sigma$ (mainly d_{z^2}) combinations (1). Excitation of $\sigma \rightarrow \sigma^*$ has been shown to dictate the photochemistry of these complexes, by inducing homolytic cleavage of the metal-metal bond (2). Our interest in the photochemistry of larger carbonyl clusters has led us to investigate the electronic structures of $M_3(CO)_{12}$ (M = Fe, Ru, Os) and $M_2Fe(CO)_{14}$ (M = Mn, Re) molecules. As photofragmentation of $Ru_3(CO)_{12}$ has been reported (3), it was of interest to us to determine whether low-lying electronic transitions similar to $\sigma \rightarrow \sigma^*$ in binuclear carbonyls would be observed in these larger clusters. Herein we report the results of our electronic spectral studies on several trinuclear carbonyl clusters. Extended Hückel molecular orbital calculations were performed on the $Ru(CO)_4$ fragment and the $Ru_3(CO)_{12}$ molecule to aid in the interpretation of the spectra.

Experimental

$Fe_3(CO)_{12}$, $Ru_3(CO)_{12}$, and $Os_3(CO)_{12}$ were purchased from Strem Chemical Co. $Fe_3(CO)_{12}$ was purified by sublimation at 60°. $Ru_3(CO)_{12}$ was recrystallized from toluene. $Os_3(CO)_{12}$ was recrystallized from benzene, and then washed dry with ether.

$Ru(CO)_5$ (3), $Ru_3(CO)_9(PPh_3)_3$ (4,5), $Ru_3(CO)_9(PEtPh_2)_3$ (4,5), $Fe_2Ru(CO)_{12}$ (6), $FeRu_2(CO)_{12}$ (6), $(PPN)MnFe_2(CO)_{12}$ (7), $Mn_2Fe(CO)_{14}$ (8), $MnFeRe(CO)_{14}$ (9), $Re_2Fe(CO)_{14}$ (10), and $Fe_2(CO)_9$ (11) were prepared by standard methods.

Electronic absorption and MCD spectra were measured on Cary 17 and Cary 61 instruments. Spectra at 77 K were obtained as described previously (1); for some measurements a Cryogenic Technology, Inc. Model 21 cryocooler was employed. The contraction of 2-methylpentane at 77 K was measured to be 22% relative to 300 K. The use of EPA and 3-PIP as glassing solvents has been described previously (1). All the low temperature spectra reported in this paper are uncorrected for solvent contraction. Techniques for obtaining band polarizations using the nematic liquid crystal solvent BPC have been described previously (12).

Thin single crystals of $Fe_3(CO)_{12}$ were grown from hexane on quartz plates. The crystals are strongly dichroic, being green in one orientation and colorless in the other. Polarized spectra were measured along the extinction directions of the crystal face. A polarized infrared spectrum was used to obtain the orientation of the $Fe_3(CO)_{12}$ molecules in the crystals. For the infrared measurements, crystals were grown on sapphire plates. Dahl and Rundle have reported (13) the polarized infrared spectrum of $Fe_3(CO)_{12}$. We found that their "|| to b" corresponded to our colorless orientation and their "|| to C_B" to our green orientation.

The orientation of the molecules in the unit cell is such that the plane of the Fe_3 triangle is nearly perpendicular to b. Thus, the green orientation is for polarized light with the electric vector in the plane of the Fe_3 triangle and the colorless orientation for the electric vector perpendicular to the Fe_3 plane.

Molecular Orbitals for $Ru(CO)_4$ and $Ru_3(CO)_{12}$

The molecular orbital energy levels for $Ru(CO)_4$ were calculated using an iterative, extended Hückel (F = 2) procedure (14). The coordinate system used is shown in Figure 1. The geometry of the fragment was idealized to C_{2v} symmetry with the angle C(1) - Ru - C(2) equal to 180° and all Ru - C - O angles also equal to 180°. The value of 100° for the angle C(3) - Ru - C(4) was taken from a crystal structure determination of $Ru_3(CO)_{12}$ (15). The bond lengths used were Ru - C_{eq} = 1.93 Å, Ru - C_{ax} = 1.89 Å, and C - O = 1.14 Å, where eq and ax refer to equatorial and axial, respectively. These values were taken from the mean bond lengths reported for $Ru_3(CO)_{12}$ (15).

The CO ligand basis set consisted of the filled 4σ, 5σ, 1π, and the unfilled 2π molecular orbitals (14). Slater atomic orbitals were used for the carbon and oxygen atomic basis set (16). The 4d, 5s, and 5p Ru atomic orbitals were taken from an earlier paper (17).

The results of the $Ru(CO)_4$ calculation are presented on the left hand side of the scheme in Figure 2 (18). Similar results

Figure 1

The coordinate system for the $Ru(CO)_4$ fragment.

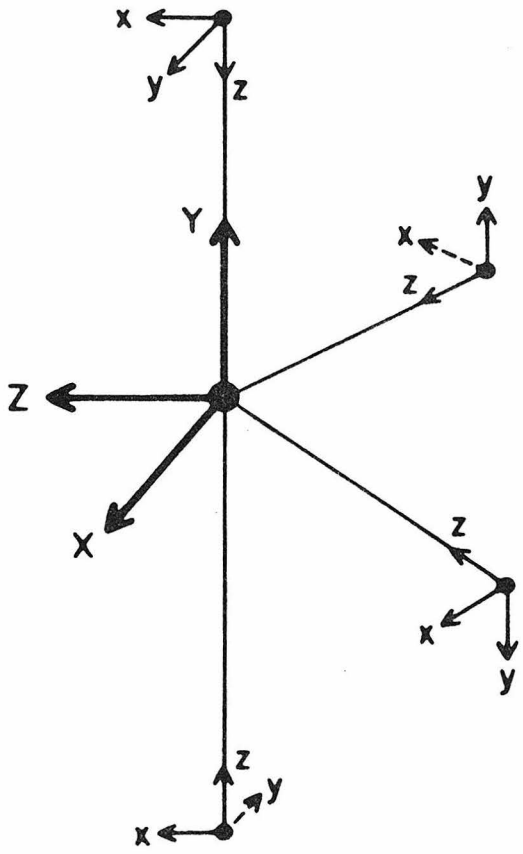
x
y
z
Y
y
x
z
Z
X
z
x
y
z
y
x

Figure 2

MO scheme for $Ru_3(CO)_{12}$. Selected energy levels for the $Ru(CO)_4$ fragment are shown at left (the $Ru(CO)_4$ HOMO is xz, and the LUMO is π^*,z).

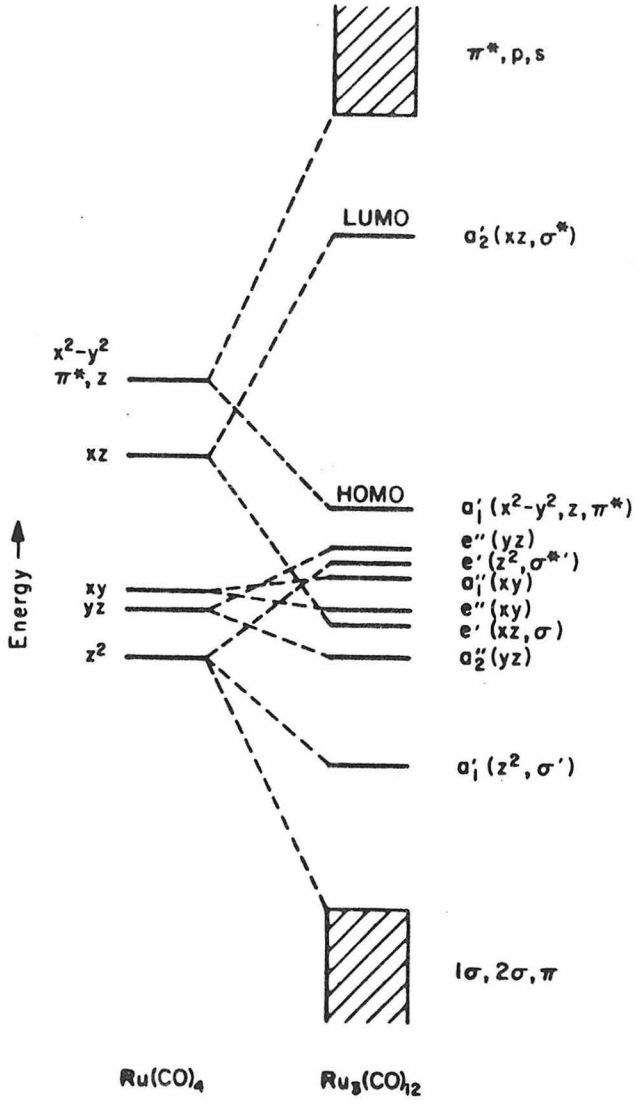
π*, p, s
LUMO
a2'(xz, σ*)
x²-y²
π*, z
xz
HOMO
a1'(x²-y², z, π*)
e''(yz)
e'(z², σ*')
a1''(xy)
e''(xy)
e'(xz, σ)
a2''(yz)
Energy
xy
yz
z²
a1'(z², σ')
1σ, 2σ, π
Ru(CO)4
Ru3(CO)12

have been obtained (19) in a calculation of the molecular orbitals of $Mn(CO)_4$. The $Ru(CO)_4$ calculation shows that there are three low-lying d orbitals that are relatively unaffected by the four CO ligands. These orbitals are directed between the ligands. Several lobes of the xz orbital are directed toward the equatorial ligands. The higher energy of this orbital reflects this antibonding character. The remaining d orbital, the $x^2 - y^2$, is directed at the axial CO ligands and, as a result, possesses extreme antibonding character. The $x^2 - y^2$ orbital is above some of the CO π^* orbitals, and it is not shown in Figure 2. The lowest unoccupied MO is a hybrid (15% $x^2 - y^2$, 25% z, 45% π^*) and is of a_1 symmetry in $Ru(CO)_4$. This orbital is involved in the metal-metal bond network when the $Ru(CO)_4$ fragments combine to form $Ru_3(CO)_{12}$.

The RuRu bond distance in $Ru_3(CO)_{12}$ was taken to be 2.848 Å (15). The F parameters used were $F_{M\sigma} = F_{\sigma\sigma} = 1.50$, $F_{M\pi} = F_{\pi\pi} = 2.2$, $F_{\sigma\,\pi} = F_{MM} = 2.0$, i.e., the same used for $Mn_2(CO)_{10}$ (1). Corrections were applied (1) to the metal orbital H_{ii} values. The calculation was not iterative due to program limitations. Thus, VSIE values for the metal H_{ii} were adjusted to those from a charge-iterative calculation on $Mo(CO)_6$ (14). These values are d = -7.4, s = -6.4, and p = -3.5 μm^{-1}.

A partial listing of the eigenvalues from the calculation is given in Table 1. These results are represented as an MO scheme in Figure 2. The metal orbitals in the cluster have been identified

Table 1. Selected Eigenvalues of $Ru_3(CO)_{12}$

-E (μm^{-1})	Symmetry	Orbital Character
3.27	e'	π^*
3.39	a_1'	π^*
3.60	e'	π^*
4.98 (LUMO)	a_2'	xz (σ^*)
6.77 (HOMO)	a_1'	$x^2 - y^2$, z, π^*
7.14	e''	yz
7.18	e'	z^2 ($\sigma^{*\prime}$)
7.20	a_1''	xy
7.41	e''	xy
7.50	e'	xz (σ)
7.73	a_2''	yz
8.32	a_1'	z^2 (σ')
10.71	a_1'	σ

by their d orbital parentage because these basis set orbitals remain relatively unmixed in the cluster. The predicted ground state is $^1A_1'(a_1'^2)$, which accords with the diamagnetism of the compound (20).

The energy levels of the metal orbitals in the $Ru_3(CO)_{12}$ cluster are determined mainly by their energies in the $Ru(CO)_4$ fragment (Figure 2). Every d atomic basis orbital in the fragment can be combined into an a-type and an e-type basis set of molecular orbitals in the cluster. Depending upon the d orbital involved, one of these molecular orbitals will be bonding and the other antibonding with respect to the metal-metal interaction. The a_1 LUMO in $Ru(CO)_4$ forms a bonding a_1' orbital in $Ru_3(CO)_{12}$; this orbital is occupied in the ground state of the trinuclear carbonyl and accounts for a significant fraction of the metal-metal bonding. The following notation is introduced to simplify the electronic spectral discussion. By analogy to $Mn_2(CO)_{10}$ (1), the e' (xz) bonding orbital is σ, whereas the a_2' (xz) antibonding orbital is σ^* (σ^* is the LUMO in $Ru_3(CO)_{12}$); the a_1' (z^2) bonding orbital is σ' and the e' (z^2) antibonding orbital is $\sigma^{*\prime}$. There are three allowed one electron transitions from the d block of molecular orbitals to σ^*; $\sigma \rightarrow \sigma^*$ ($^1A_1' \rightarrow {}^1E'$), $\sigma^{*\prime} \rightarrow \sigma^*$ ($^1A_1' \rightarrow {}^1E'$), and a_1'' (xy) $\rightarrow$ $\sigma^*(^1A_1' \rightarrow {}^1A_2'')$.

Electronic Spectra

The electronic spectra of $Ru_3(CO)_{12}$ at 300 and 77 K are shown in Figure 3. The most interesting feature is an intense band at

Figure 3

Electronic absorption spectra of $Ru_3(CO)_{12}$ in 2-methylpentane at 300 and 77 K.

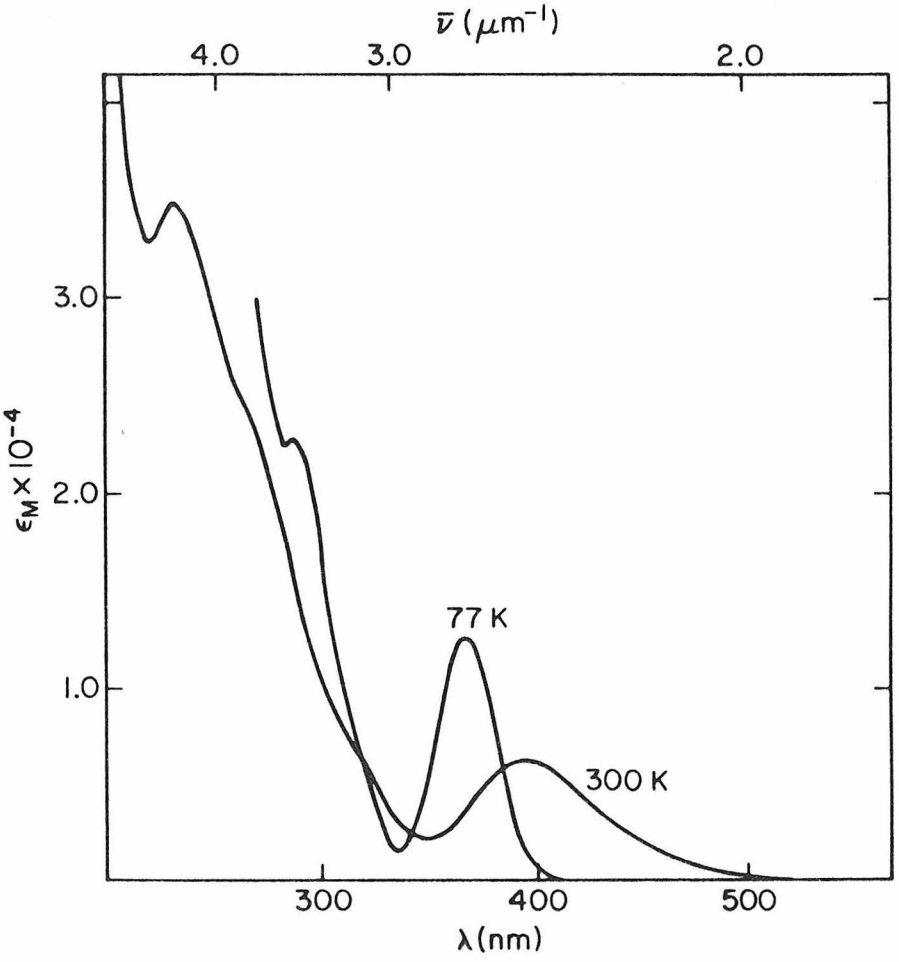
$\bar{\nu}$ (μm^{-1})
4.0
3.0
2.0
3.0
2.0
1.0
$\epsilon_M \times 10^{-4}$
77 K
300 K
300
400
500
λ(nm)

390 nm (2.56 μm^{-1}) that sharpens and blue shifts markedly upon cooling. In the nematic liquid crystal solvent BPC, the 2.56 μm^{-1} band is in-plane (X-Y) polarized (Table 2). This means that the transition must be either $\sigma \rightarrow \sigma^*$ or $\sigma^{*\prime} \rightarrow \sigma^*$, either of which gives an E' excited state and is thus X-Y polarized. The A term in the MCD spectrum of this band confirms the degeneracy of the excited state (Table 2). According to the calculation, the $\sigma^{*\prime}$ orbital is higher in energy than the σ orbital (Figure 2). However, the calculated energy separation between the $\sigma^{*\prime}$ and σ orbitals is too small (0.32 μm^{-1}) to predict with any confidence which of the $^1A_1' \rightarrow {}^1E'$ transitions lies to lower energy. In order to decide this question, we found it necessary to examine the spectra of several closely-related derivatives.

The spectra of $Ru_3(CO)_9(PEtPh_2)_3$ at 300 and 77 K are shown in Figure 4. Spectral data for other $Ru_3(CO)_9(PR_3)_3$ complexes are given in Table 2. All these complexes have bands near 390 nm (~2.6 μm^{-1}) that sharpen and blue shift on cooling. But, unlike $Ru_3(CO)_{12}$, the phosphine-substituted complexes have an additional band near 500 nm (~2.0 μm^{-1}). Since phosphine substitution occurs at a site that is in the Ru_3 plane, it is the energy of the xz orbital that is primarily affected (Figure 5). Replacement of CO by a phosphine makes the xz orbital less antibonding. This means that the xz - z^2 energy separation in the $Ru(CO)_3(PR_3)$ fragment will be less than in the $Ru(CO)_4$ fragment. As a result

Table II. Electronic Spectral Data[a] and Transition Assignments

complex	300 K			77 K			MCD		
	λ_{max}, nm	$\bar{\nu}_{max}$, μm^{-1}	$\epsilon_M \times 10^{-4}$	λ_{max}, nm	$\bar{\nu}_{max}$, μm^{-1}	$\epsilon_M \times 10^{-4}$	polarization	A term	assignment
$Ru_3(CO)_{12}$	390	2.56	0.64	367	2.72	1.02	in-plane[b]	379	$\sigma \rightarrow \sigma^*$
	320 sh	3.12		320 sh	3.12			305	$\sigma^{*\prime} \rightarrow \sigma^*$
				292	3.42	1.50			
	270 sh	3.70							
	238	4.20	3.50						MLCT
$Os_3(CO)_{12}$	385 sh	2.60	0.36	381	2.62	0.56		385	$\sigma^{*\prime} \rightarrow \sigma^*$
	330	3.03	0.86	317	3.15	2.06		327	$\sigma \rightarrow \sigma^*$
	280 sh	3.57		275 sh	3.64	1.30			
	240	4.17	2.48						MLCT
$Fe_3(CO)_{12}$	602	1.66	0.32	605	1.65	0.52	in-plane		$\sigma^{*\prime} \rightarrow \sigma^*$
	437 sh	2.29		435	2.30	0.48	in-plane		$\sigma \rightarrow \sigma^*$
	360 sh	2.78		360 sh	2.78				
	310 sh	3.22		320 sh	3.12				
				297	3.37	1.85			
	263	3.80	3.00						MLCT
$FeRu_2(CO)_{12}$	470 sh	2.13		468	2.17	0.70			$\sigma^{*\prime} \rightarrow \sigma^*$
	390	2.56	0.88	368	2.72	1.28			$\sigma \rightarrow \sigma^*$
$Ru_3(CO)_9(PEtPh_2)_3$[c]	492	2.03	1.15	495	2.02	1.59		487	$\sigma^{*\prime} \rightarrow \sigma^*$
	370	2.70	1.22	353	2.83	1.54		372	$\sigma \rightarrow \sigma^*$
$Ru_3(CO)_9(PPh_3)_3$[c]	507	1.97	1.23	520	1.92	1.88		501	$\sigma^{*\prime} \rightarrow \sigma^*$
	387	2.58	1.28	375	2.67	2.00		394	$\sigma \rightarrow \sigma^*$
$Mn_2Fe(CO)_{14}$[d]	431	2.32	2.38	424	2.36	4.01			$\sigma \rightarrow \sigma^*$
$Re_2Fe(CO)_{14}$	380	2.63	3.00	379	2.64	4.82	ReFeRe axis		$\sigma \rightarrow \sigma^*$
$MnFeRe(CO)_{14}$	403	2.48							$\sigma \rightarrow \sigma^*$
$Ru(CO)_5$	260 sh	3.85	0.57						$e' \rightarrow a'_1$
	236	4.24	0.84						MLCT

[a] In 2-methylpentane unless noted otherwise. [b] R. A. Levenson, Ph.D. Thesis, Columbia University, 1970. [c] In EPA. [d] In 3-PIP.

Figure 4

Electronic absorption spectra of $Ru_3(CO)_9(PEtPh_2)_3$ in EPA at 300 and 77 K.

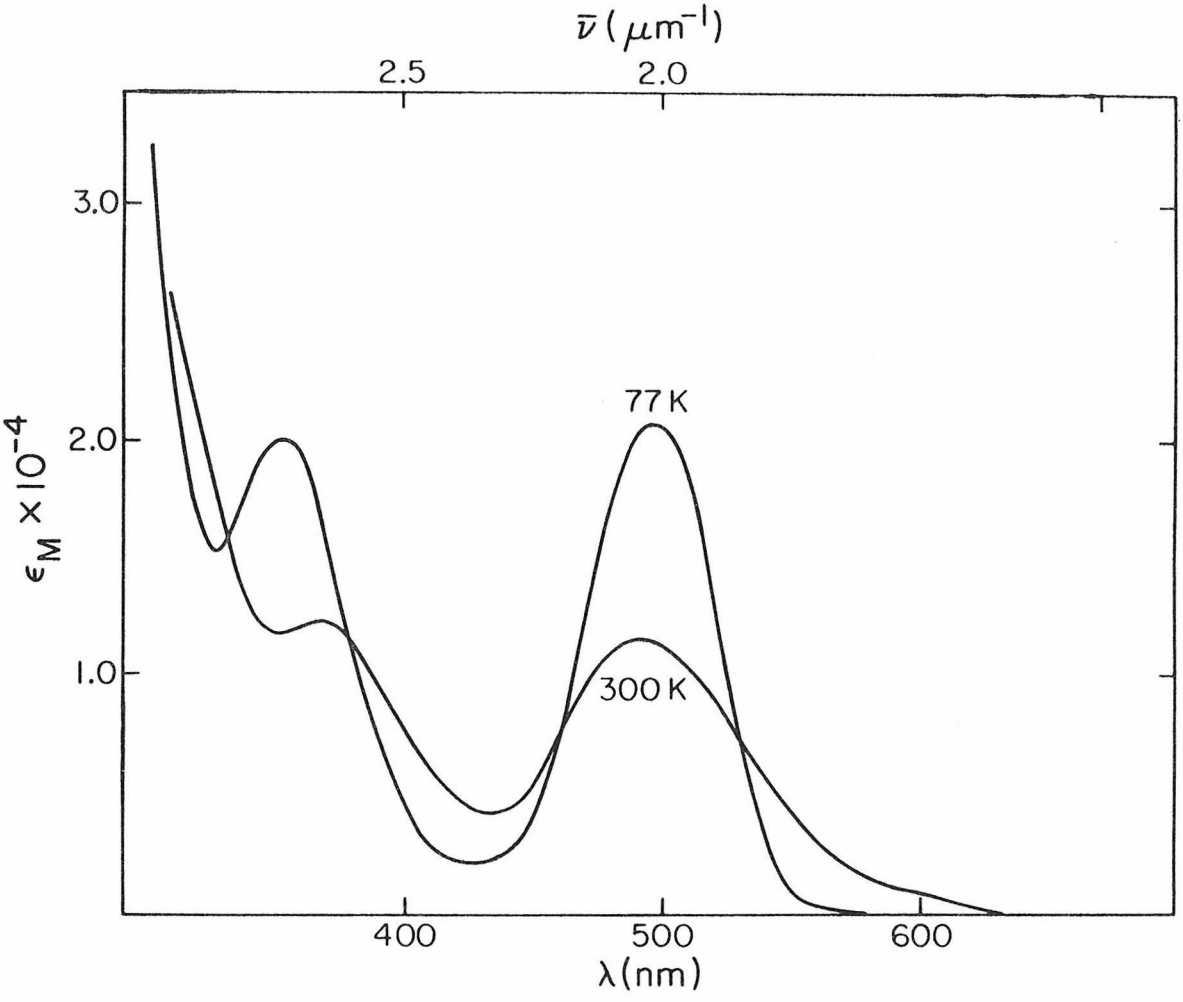
$\bar{\nu}$ (μm^{-1})
2.5
2.0
3.0
2.0
1.0
$\epsilon_M \times 10^{-4}$
77 K
300 K
400
500
600
λ(nm)

Figure 5

Schematic of the interactions of xz and z^2 fragment orbitals to form trimer cluster orbitals (σ',$\sigma^{*'}$,σ,σ^*): (a) proposed interaction scheme for $Ru_3(CO)_{12}$; (b) the effect of increased metal-metal overlap on the σ and $\sigma^{*'}$ orbital energies, as proposed for $Os_3(CO)_{12}$; and (c) the effect of decreased z^2 - xz energy separation on the σ and $\sigma^{*'}$ orbital energies, as proposed for $Ru_3(CO)_9(PR_3)_3$.

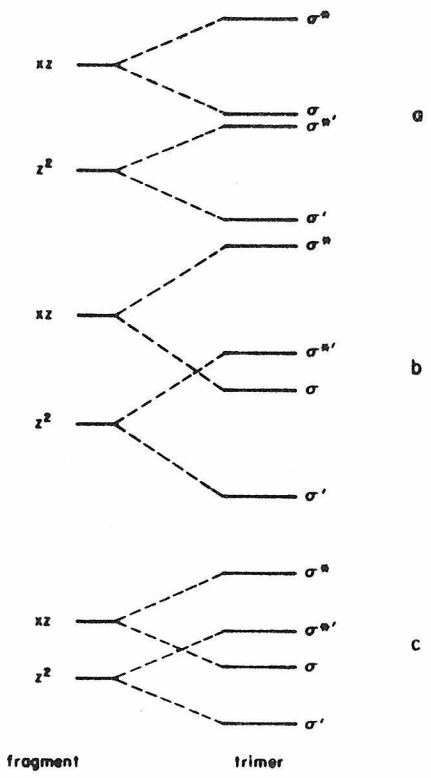
xz
z²
xz
z²
xz
z²
σ*
σ
σ*'
σ'
σ*
σ*'
σ
σ'
σ*
σ*'
σ
σ'
a
b
c
fragment
trimer

of the decreased separation, when the fragments combine to form the trimer, the z^2 antibonding orbital ($\sigma^{*\prime}$) is higher in energy than the xz bonding orbital. Thus, the energy of the $\sigma^{*\prime} \rightarrow \sigma^*$ transition should decrease on going from $Ru_3(CO)_{12}$ to $Ru_3(CO)_9(PR_3)_3$. Accordingly, the "new" band at ~2.0 μm^{-1} in the $Ru_3(CO)_9(PR_3)_3$ complexes is assigned to the $\sigma^{*\prime} \rightarrow \sigma^*$ transition. Both the ~2.0 and ~2.6 μm^{-1} bands exhibit MCD A terms (Figure 6), which is consistent with our assignment.

The above interpretation of the $Ru_3(CO)_9(PR_3)_3$ spectrum suggests an assignment for the 2.56 μm^{-1} band in $Ru_3(CO)_{12}$. In addition to having nearly the same energy, this band has the same temperature-dependent behavior (sharpening and blue-shifting on cooling) as the ~2.6 μm^{-1} band in the $Ru_3(CO)_9(PR_3)_3$ complexes. These similarities suggest that the same transition is involved in each case and hence the 2.56 μm^{-1} band is assigned to $\sigma \rightarrow \sigma^*$ in the $Ru_3(CO)_{12}$ molecule. We note that this $\sigma \rightarrow \sigma^*$ assignment is consistent with the interpretation of the spectra of binuclear metal carbonyls (1). The observed temperature dependence of the band shape in $M_2(CO)_{10}$ molecules is related to the substantial depopulation of excited M_2 vibrational levels that occurs upon cooling the molecule to 77 K (1). Similar temperature-dependent behavior is expected for $\sigma \rightarrow \sigma^*$ bands in trinuclear clusters, as the electronic transition will be coupled to the low-frequency M_3 stretching motions in these molecules.

Phosphine substitution lowers the energy of the $\sigma \rightarrow \sigma^*$ transition in $Mn_2(CO)_{10}$. Thus, it is possible that the band

Figure 6

MCD spectrum of $Ru_3(CO)_9(PEtPh_2)_3$ in 2-methylpentane at 25° C. The ordinate is in units of ellipticity $gauss^{-1}$. 10^4 wavenumbers (cm^{-1}) = 1 μm^{-1}.

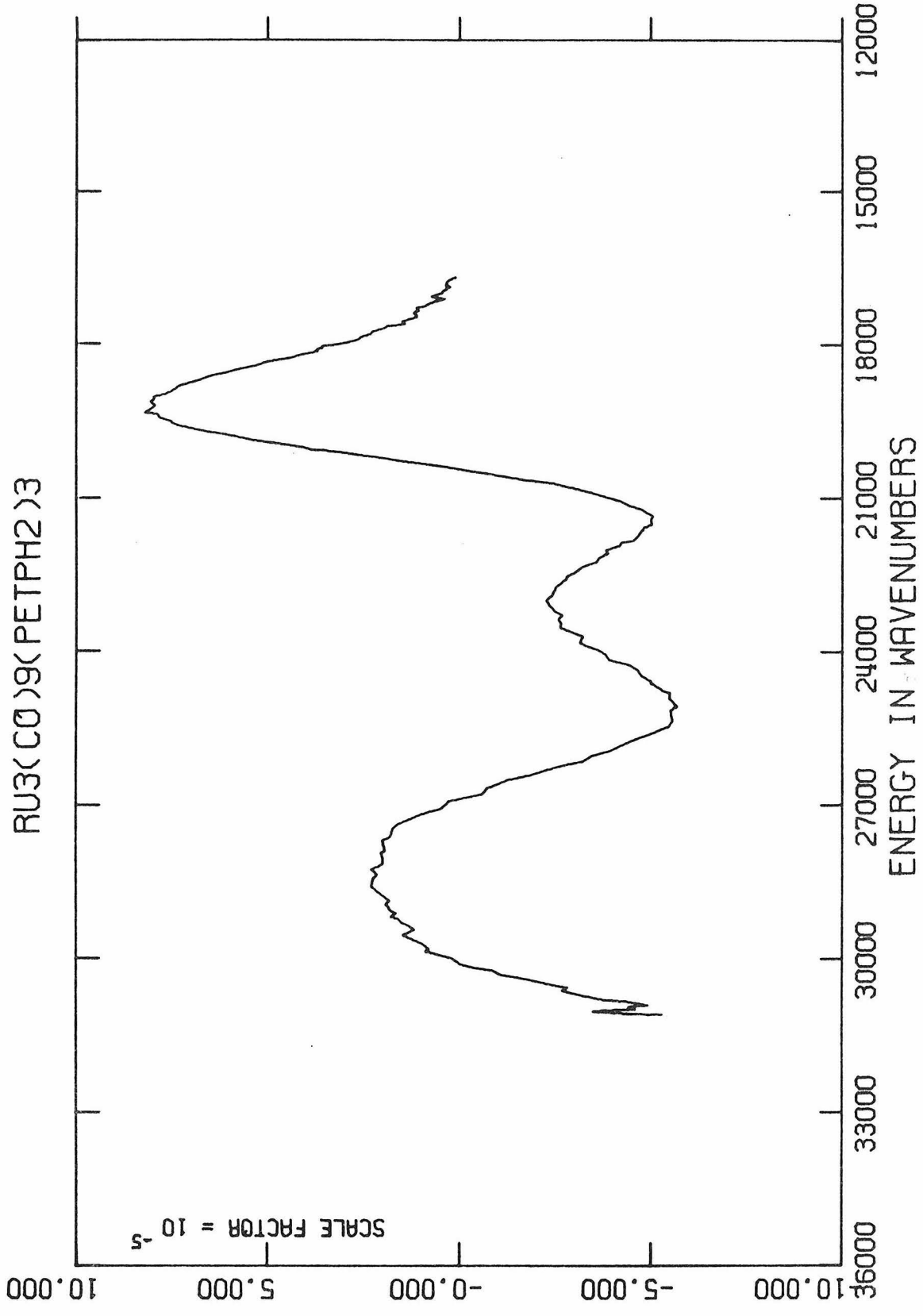
RU3(CO)9(PETPH2)3
10.000
5.000
-0.000
-5.000
-10.000
SCALE FACTOR = 10 -5
36000
33000
30000
27000
24000
21000
18000
15000
12000
ENERGY IN WAVENUMBERS

assignments above are reversed, that is, phosphine substitution has shifted the $\sigma \rightarrow \sigma^*$ transition from 2.56 μm^{-1} in $Ru_3(CO)_{12}$ to ~2.00 μm^{-1} in $Ru_3(CO)_9(PR_3)_3$. Two lines of evidence suggest that the latter has not happened. Firstly, the shifts in the $Mn_2(CO)_{10}$ $\sigma \rightarrow \sigma^*$ transition energy with phosphine substitution are much smaller than 0.56 μm^{-1} (2.56 to 2.00 μm^{-1}). Secondly, on cooling, the ~2.6 μm^{-1} band sharpens and blue shifts, as is characteristic of a $\sigma \rightarrow \sigma^*$ transition.

Spectra of several $Ru_3(CO)_9(ER_3)_3$ (E = P, As, Sb) derivatives show that the lowest band increases in energy according to $PPh_3 < PEtPh_2 < PEt_2Ph < PEt_3$ (and also $PPh_3 < AsPh_3 < SbPh_3$) (5), following the σ-donor ability of the ligands. With increasing σ-donor ability, the $d_{z^2} - d_{xz}$ ligand field splitting increases in any given monomeric fragment, with a corresponding increase in energy for the $\sigma^{*\prime} \rightarrow \sigma^*$ transition in the trimer. We also note that the colors of the compounds $M_3(CO)_{11}PR_3$, $M_3(CO)_{10}(PR_3)_2$, and $M_3(CO)_9(PR_3)_3$ (M = Ru, Os) are generally yellow, orange, and red, respectively (21). Increasing phosphine substitution likely results in a decrease in the average $d_{z^2} - d_{xz}$ (fragment) ligand field splitting, thereby lowering the energy of the $\sigma^{*\prime} \rightarrow \sigma^*$ transition in the trinuclear molecules.

Electronic absorption spectral data for $Os_3(CO)_{12}$ are summarized in Table 2. The peak at 330 nm (3.03 μm^{-1}) and the shoulder at 385 nm (2.60 μm^{-1}) give rise to MCD A terms (Figure 7), indicating

Figure 7

MCD spectrum of $Os_3(CO)_{12}$ in 2-methylpentane at 25° C. The ordinate is in units of ellipticity $gauss^{-1}$. 10^4 wavenumbers (cm^{-1}) = 1 μm^{-1}.

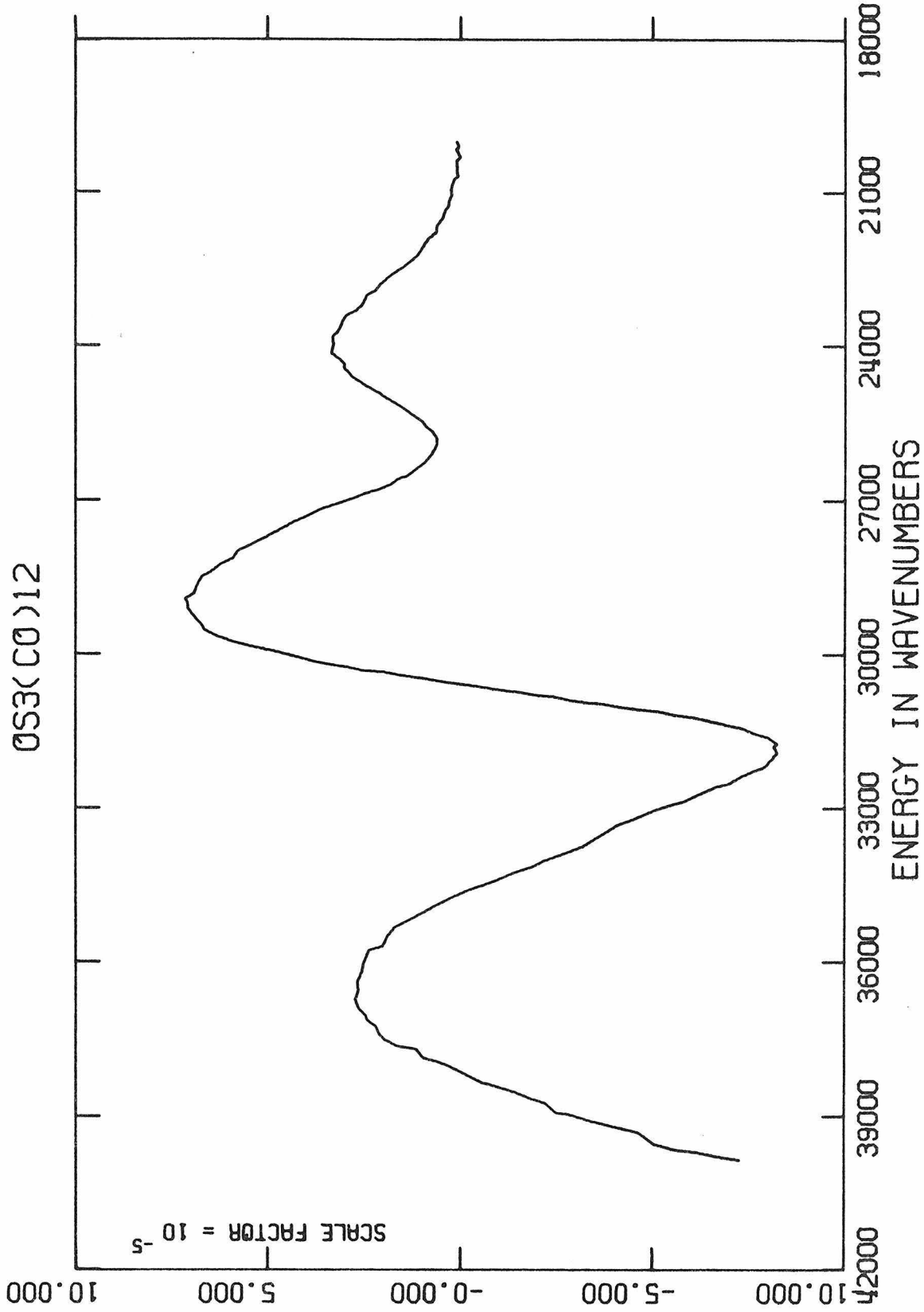
Os3(CO)12
SCALE FACTOR = 10 -5
10.000
5.000
-0.000
-5.000
-10.000
42000
39000
36000
33000
30000
27000
24000
21000
18000
ENERGY IN WAVENUMBERS

degenerate excited states. The band at 3.03 μm^{-1} sharpens and blue shifts, and is assigned to $\sigma \rightarrow \sigma^*$. The weaker band at 2.60 μm^{-1} is assigned to $\sigma^{*\prime} \rightarrow \sigma^*$, which is the other low-lying transition to a degenerate excited state.

The $\sigma \rightarrow \sigma^*$ transition was assigned to the lowest energy band in $Ru_3(CO)_{12}$; however, in $Os_3(CO)_{12}$, the $\sigma^{*\prime} \rightarrow \sigma^*$ transition is below $\sigma \rightarrow \sigma^*$. We suggest that this pattern of relative transition energies is reasonable because the metal-metal orbital interactions should be greater in $Os_3(CO)_{12}$ than in $Ru_3(CO)_{12}$, causing a greater bonding-antibonding energy splitting in the former molecule. As a result, in $Os_3(CO)_{12}$ the z^2 antibonding MO($\sigma^{*\prime}$) moves above the xz bonding orbital (σ), as shown in Figure 5b, and the $\sigma \rightarrow \sigma^*$ transition occurs at higher energy ($Ru_3(CO)_{12}$, 2.56 μm^{-1} < $Os_3(CO)_{12}$, 3.05 μm^{-1}). The $\sigma^{*\prime} \rightarrow \sigma^*$ transition therefore falls at lower energy than $\sigma \rightarrow \sigma^*$ in $Os_3(CO)_{12}$. Independent evidence that the metal-metal interactions are stronger in $Os_3(CO)_{12}$ than in $Ru_3(CO)_{12}$ comes from stretching force constants, which are 0.91 mdyn/Å for the former molecule and 0.82 mdyn/Å for the latter (22). A similar correlation of $\sigma \rightarrow \sigma^*$ transition energies and stretching force constants has been noted (1) for $M_2(CO)_{10}$ (M = Mn, Tc, Re) molecules.

The spectral data for $Os_3(CO)_{12}$ show that the $\sigma^{*\prime} \rightarrow \sigma^*$ band is much weaker than that associated with the $\sigma \rightarrow \sigma^*$ transition. Careful inspection of the $Ru_3(CO)_{12}$ spectrum reveals a weak band, which appears as a shoulder at 3.12 μm^{-1}, and the MCD spectrum of

the molecule (Table 2) indicates the presence of an A term positioned at 305 nm (3.20 μm^{-1}). We propose, therefore, that the weak band at 3.12 μm^{-1} in $Ru_3(CO)_{12}$ is attributable to $\sigma^{*\prime} \rightarrow \sigma^*$.

We turn next to the spectrum of $FeRu_2(CO)_{12}$, which possesses a triangular $FeRu_2$ cluster and only terminal CO groups in solution (6). A band at 390 nm (2.56 μm^{-1}) in the spectrum of this molecule (Table 2) blue shifts and sharpens upon cooling. Owing to this characteristic temperature-dependent behavior, this band is assigned to the $\sigma \rightarrow \sigma^*$ transition. The weaker band at 470 nm (2.13 μm^{-1}) is assigned to the $\sigma^{*\prime} \rightarrow \sigma^*$ transition. The presence of Fe in the $FeRu_2$ triangle decreases the average ligand field splitting of the xz and z^2 orbitals (Figure 5c), thereby placing the $\sigma^{*\prime}$ orbital above σ, as in the case of $Ru_3(CO)_9L_3$. Consequently, the $\sigma^{*\prime} \rightarrow \sigma^*$ transition falls lower than $\sigma \rightarrow \sigma^*$.

Electronic absorption spectral data for $Fe_3(CO)_{12}$ are given in Table 2. If the symmetry of CO-bridged $Fe_3(CO)_{12}$ is idealized to C_{2v}, then the $\sigma \rightarrow \sigma^*$ and $\sigma^{*\prime} \rightarrow \sigma^*$ (both $e' \rightarrow a_2'$) transitions are no longer $^1A_1' \rightarrow {}^1E'$, but are split into two transitions, $^1A_1 \rightarrow {}^1A_1$ and $^1A_1 \rightarrow {}^1B_1$. Both transitions are polarized in the plane of the triangle, one component of each in the Z (C_{2v}) direction ($^1A_1 \rightarrow {}^1A_1$) and the other in the X (C_{2v}) direction ($^1A_1 \rightarrow {}^1B_1$). Spectroscopic measurements on a single crystal of $Fe_3(CO)_{12}$ clearly show that the two lowest energy bands are polarized in the plane of the Fe_3 triangle (Figure 8). Dahl and

Figure 8

Single crystal polarized electronic absorption spectra of $Fe_3(CO)_{12}$ at 25° C. The spectra are for the electric vector of light perpendicular to the Fe_3 plane ($\perp$) and in the plane ($\parallel$).

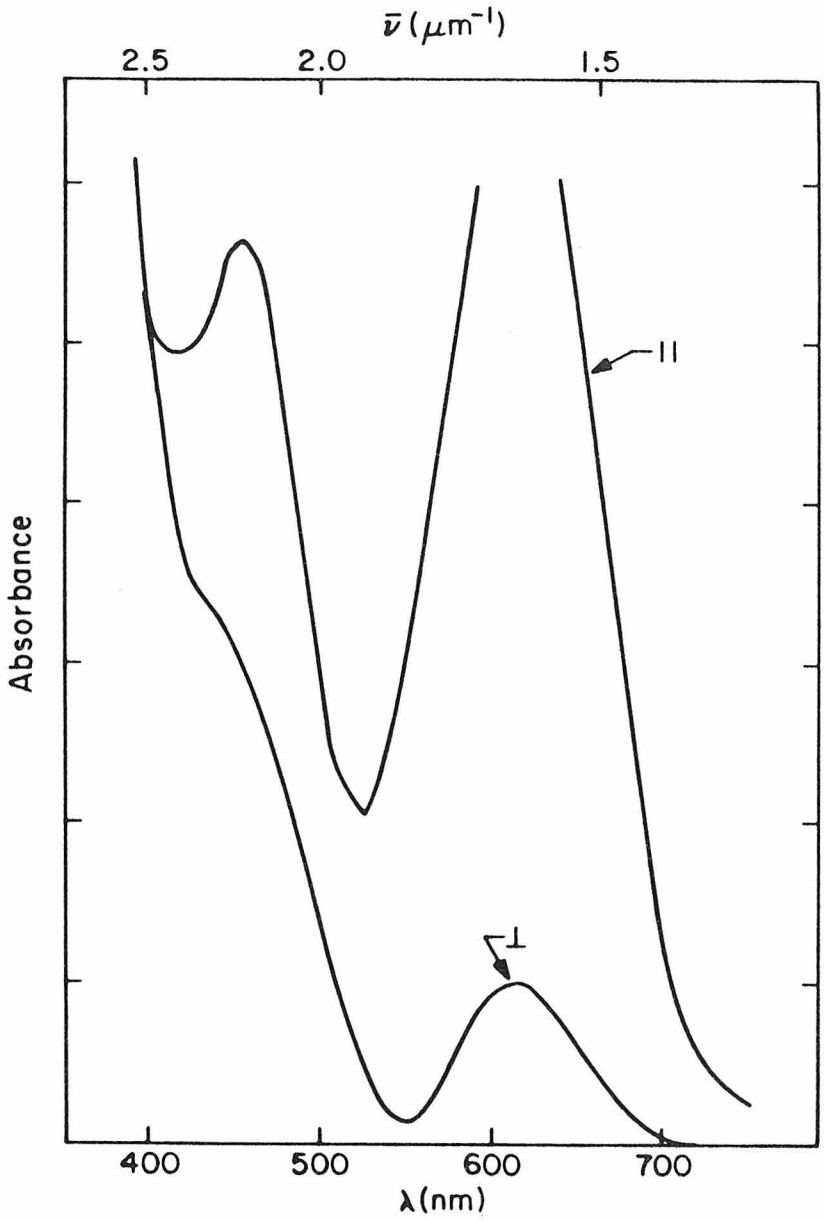
$\bar{\nu}$ (μm^{-1})
2.5
2.0
1.5
Absorbance
||
⊥
400
500
600
700
λ(nm)

Rundle have discussed the disordering of the $Fe_3(CO)_{12}$ molecules in the unit cell (13). It is this disorder that prevents us from distinguishing the Z and X polarizations. However, even our glass spectra at 77 K revealed no splitting of either the 602 (1.66) or the 437 nm (2.29 μm^{-1}) band.

As in the other $M_3(CO)_{12}$ molecules and consistent with the polarization data, we assign the two lowest energy bands in $Fe_3(CO)_{12}$ to the $\sigma \rightarrow \sigma^*$ and $\sigma^{*\prime} \rightarrow \sigma^*$ transitions. However, it is possible that one or both of these bands are low-energy charge transfer transitions involving the bridging CO ligands. To examine this possibility, we studied the electronic spectrum of $Fe_2(CO)_9$, a molecule with three bridging CO groups. The spectrum showed only rising absorption into the UV with no bands of appreciable intensity in the visible region. Likewise, our study of the electronic spectrum of $Co_2(CO)_8$ did not reveal any bands in the visible region attributable to metal $\rightarrow$ bridging-CO transitions (23). Further evidence that the two low energy transitions in $Fe_3(CO)_{12}$ are not charge transfer is provided by the spectrum of $(PPN)MnFe_2(CO)_{12}$. The cluster structure of $MnFe_2(CO)_{12}^-$ is the same (7) as that of $Fe_3(CO)_{12}$. The spectra of the two complexes are similar except that the two lowest energy transitions in $MnFe_2(CO)_{12}^-$ (1.74, 2.86 μm^{-1}) are blue-shifted with respect to their counterparts in $Fe_3(CO)_{12}$ (1.66, 2.29 μm^{-1}). Substitution of Mn(-I) for Fe(0) should red shift metal-to-ligand charge transfer (MLCT) transitions.

Such a shift has been observed for the MLCT transitions when Cr(-I) is substituted for Mn in $Mn_2(CO)_{10}$ (1). Thus, it is unlikely that the two lowest energy bands in $Fe_3(CO)_{12}$ are due to MLCT transitions.

It remains to assign the $\sigma \rightarrow \sigma^*$ and $\sigma^{*\prime} \rightarrow \sigma^*$ transitions in $Fe_3(CO)_{12}$. For this, a comparison of the spectra of the complexes in the series $Fe_nRu_{3-n}(CO)_{12}$ (n = 0-3) is useful (Table 3). We discussed above why the $\sigma^{*\prime} \rightarrow \sigma^*$ transition is lower in energy than $\sigma \rightarrow \sigma^*$ in $FeRu_2(CO)_{12}$. Upon substitution of another Fe for Ru to give $Fe_2Ru(CO)_{12}$, the $\sigma^{*\prime} \rightarrow \sigma^*$ transition should fall to even lower energy. Indeed, the lowest energy band is now at 1.79 μm^{-1} in comparison to 2.13 μm^{-1} in $FeRu_2(CO)_{12}$. The band is at lower energy still in $Fe_3(CO)_{12}$ (1.66 μm^{-1}). Thus, the $\sigma^{*\prime} \rightarrow \sigma^*$ transition energy decreases as the average splitting of the xz and z^2 orbitals decreases. The $\sigma \rightarrow \sigma^*$ transition is assigned to the 2.29 μm^{-1} band. This band is unresolved in solution at room temperature, so it is difficult to determine if the band blue-shifts and sharpens on cooling. However, we note that the 1.66 μm^{-1} band red-shifts on cooling, which indicates that a $\sigma \rightarrow \sigma^*$ transition is not involved.

Charge Transfer Bands

Metal-to-ligand charge transfer transitions in metal carbonyls generally fall in the ultraviolet region of the spectrum (1). The energies of such transitions are mainly determined (1) by the nature of the central metal atom, i.e., the positions of d(Fe) $\rightarrow \pi^*$CO and

Table 3. Comparison of Band Positions in the Series $Fe_nRu_{3-n}(CO)_{12}$ (n = 0-3)

Complex	$\sigma \rightarrow \sigma^*$, μm^{-1} ($\varepsilon_M \times 10^{-4}$[a]; f[b])	$\sigma^{*\prime} \rightarrow \sigma^*$, μm^{-1} ($\varepsilon_M \times 10^{-4}$[a]; f[b])
$Ru_3(CO)_{12}$	2.72 (1.02; 0.13)	3.12 (cannot be measured)
$FeRu_2(CO)_{12}$	2.72 (1.28; 0.18)	2.13 (0.70; 0.06)
$Fe_2Ru(CO)_{12}$	2.63 (0.86; 0.15)	1.79 (0.68; 0.07)
$Fe_3(CO)_{12}$	2.29 (0.48; 0.04)	1.66 (0.52; 0.08)

[a] 77 K.

[b] Oscillator strength (f) as defined in Ref. 1.

d(Ru) → π*CO charge transfers in $Fe_3(CO)_{12}$ and $Ru_3(CO)_{12}$ may be reasonably estimated from the MLCT band energies observed for $Fe(CO)_5$ and $Ru(CO)_5$, respectively. The lowest MLCT band in the spectrum of $Fe(CO)_5$ falls at 242 nm (4.13 μm^{-1}) (24), whereas that in $Ru(CO)_5$ occurs at 236 nm (4.24 μm^{-1}) (Table 2). Thus, we assign the intense bands at 263 nm (3.80 μm^{-1}) in $Fe_3(CO)_{12}$ and at 238 nm (4.20 μm^{-1}) in $Ru_3(CO)_{12}$ to MLCT transitions. By analogy, the band at 240 nm (4.17 μm^{-1}) in the spectrum of $Os_3(CO)_{12}$ is attributed to a similar MLCT transition.

D_{4h} $M_2Fe(CO)_{14}$ Complexes

Figure 9 illustrates the proposed MO scheme for D_{4h} (25) $M_2Fe(CO)_{14}$-type (M = Mn, Re) molecules. If Z is taken as the internuclear axis, then metal-metal bonding is expected to involve mainly the d_{z^2} orbitals. The $3d_{z^2}$ orbital on Fe transforms as a_{1g}; thus, in the trinuclear molecule the Fe $3d_{z^2}$ interacts with the M_2 a_{1g} combination to form bonding and antibonding molecular orbitals. The M_2 a_{2u} combination is stabilized by interaction with the Fe $4p_z$ orbital.

The d_{xz}, d_{yz}, and d_{xy} orbitals, which are of π or δ symmetry in $M_2Fe(CO)_{14}$, lie to lower energy. As the overlaps between the π or δ orbitals on different metal atoms are small, these orbitals will lie below the d_{z^2} levels in the trinuclear molecules. The $d_{x^2-y^2}$ orbitals are strongly antibonding with respect to the CO

Figure 9

MO scheme for a D_{4h} $M_2Fe(CO)_{14}$ molecule.

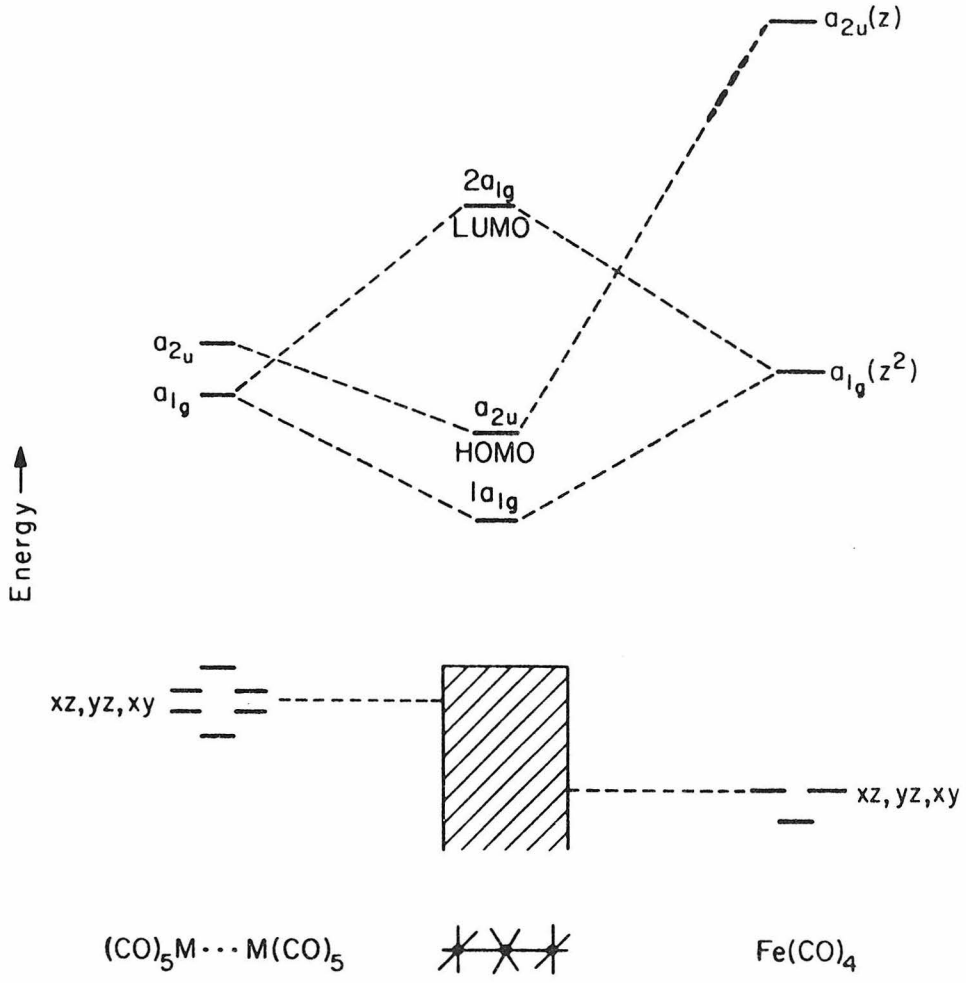
$a_{2u}(z)$
$2a_{1g}$
LUMO
a_{2u}
a_{1g}
$a_{1g}(z^2)$
a_{2u}
HOMO
$1a_{1g}$
Energy
xz, yz, xy
xz, yz, xy
$(CO)_5M\cdots M(CO)_5$
$Fe(CO)_4$

donor orbitals; hence, they are higher in energy than the d_{z^2} levels. Thus, of the 22 d valence electrons in $M_2Fe(CO)_{14}$, 18 occupy the low-lying $d\pi$ and $d\delta$ orbitals, and the remaining 4 electrons fill the bonding a_{1g} and a_{2u} molecular orbitals. The ground state is $^1A_{1g}(1a_{1g}^2 a_{2u}^2)$.

The crystal structure determination (24) of $Mn_2Fe(CO)_{14}$ provides evidence that the mixing of the M_2 a_{2u} combination with the Fe $4p_z$ orbital is important. Without such interaction, the a_{2u} level would be nonbonding, implying weak metal-metal bonds relative to $Mn_2(CO)_{10}$. However, the MnFe bond length is 2.81 Å (25), which is slightly shorter than the MnMn bond length of 2.92 Å in $Mn_2(CO)_{10}$ (26).

The lowest allowed electronic excitation is predicted to be $^1A_{1g} \rightarrow {}^1A_{2u}$ ($a_{2u} \rightarrow 2a_{1g}$), which is a $\sigma \rightarrow \sigma^*$ transition. This transition should be polarized along the MFeM(Z) axis. Note that the $1a_{1g} \rightarrow 2a_{1g}$ transition is not allowed. The spectra of $Re_2Fe(CO)_{14}$ at 300 and 77 K are shown in Figure 10. We have found that the lowest energy band in $Re_2Fe(CO)_{14}$ is polarized along the ReFeRe axis in the nematic liquid crystal solvent BPC (Figure 11). This finding is consistent with a $\sigma \rightarrow \sigma^*$ ($a_{2u} \rightarrow 2a_{1g}$) assignment for the band in question. A similar assignment is made for the intense lowest energy band in $Mn_2Fe(CO)_{14}$ (Table 2). The $\sigma \rightarrow \sigma^*$ band in $MnFeRe(CO)_{14}$ (2.48 μm^{-1}) falls between those of $Mn_2Fe(CO)_{14}$ (2.32 μm^{-1}) and $Re_2Fe(CO)_{14}$ (2.63 μm^{-1}).

Figure 10

Electronic absorption spectra of $Re_2Fe(CO)_{14}$ in 3-PIP at 300 and 77 K.

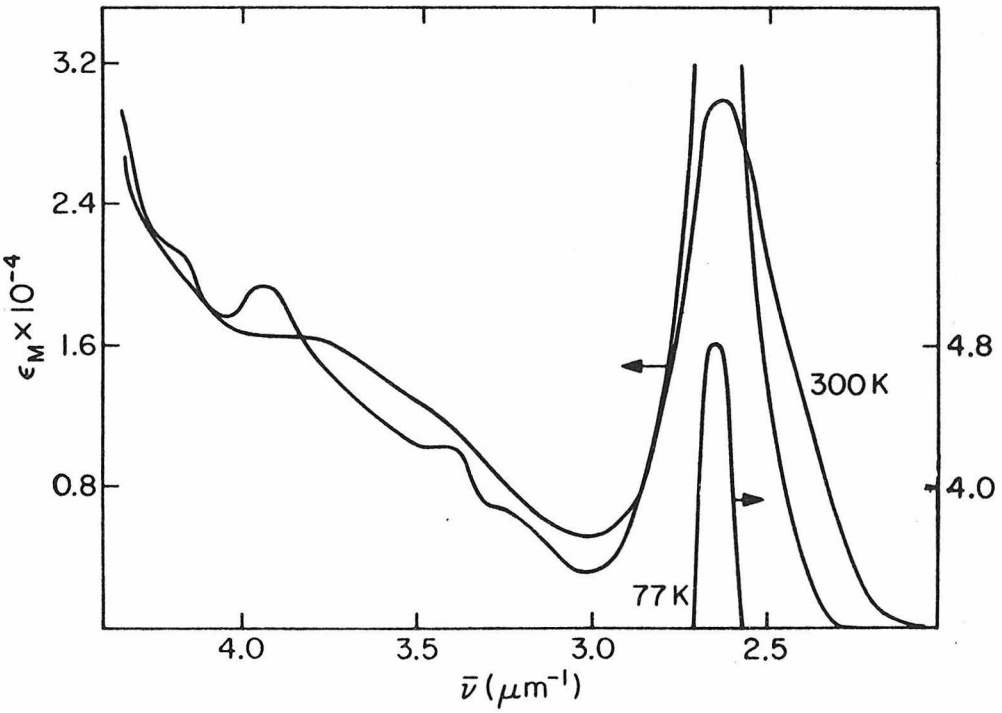
3.2
2.4
1.6
0.8
$\epsilon_M \times 10^{-4}$
4.8
4.0
300 K
77 K
4.0
3.5
3.0
2.5
$\bar{\nu}$ (μm^{-1})

Figure 11

Polarized spectra of $Re_2Fe(CO)_{14}$ in BPC; the spectra are corrected for the absorption of BPC and are for the electric vector of light polarized parallel (||) and perpendicular ($\underline{|}$) to the long axis of the oriented BPC molecules (see Ref. 12).

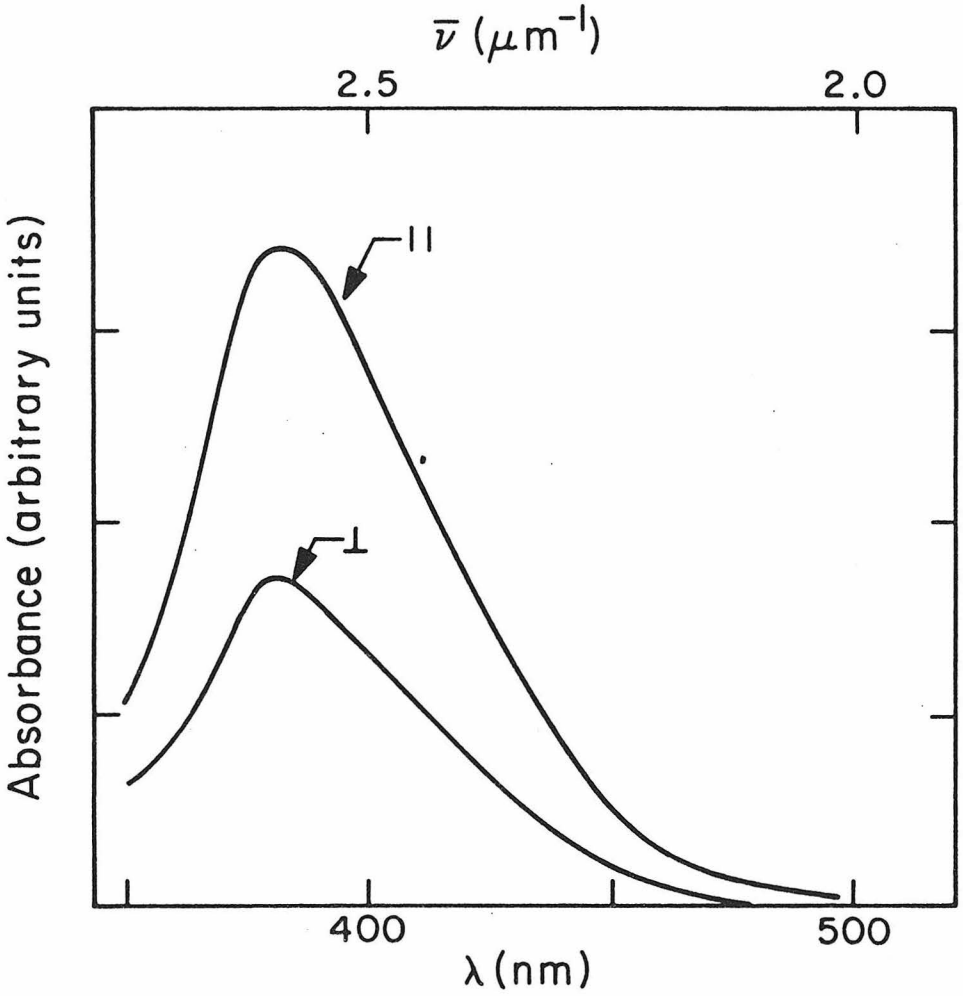
$\bar{\nu}$ (μm^{-1})
2.5
2.0
Absorbance (arbitrary units)
||
⊥
400
500
λ (nm)

The energy of the $a_{2u} \rightarrow 2a_{1g}$ band maximum increases by about 0.4 μm^{-1} in $Mn_2Fe(CO)_{14}$ on going from 300 to 77 K, whereas in $Re_2Fe(CO)_{14}$, it blue-shifts 0.1 μm^{-1}. This characteristic behavior of a $\sigma \rightarrow \sigma^*$ band has now been demonstrated for $M_2(CO)_{10}^-$ (1), $M_2(CO)_8^-$ (23), $M_3(CO)_{12}^-$, and $M_4(CO)_{12}^-$ (27) type compounds and their derivatives.

Acknowledgment

We thank David M. Dooley for assistance with certain of the MCD spectroscopic measurements. This research was supported by the National Science Foundation (CHE75-19086).

Supplementary Material Available: Listing of basis functions, eigenvectors, and eigenvalues for $Ru(CO)_4$ and $Ru_3(CO)_{12}$ (29 pages). Ordering information is given on any current masthead page.

References and Notes

1. R. A. Levenson and H. B. Gray, J. Am. Chem. Soc., 97, 6042 (1975).
2. M. S. Wrighton, Topics in Current Chemistry, 65, 37 (1975).
3. B. F. G. Johnson, J. Lewis, and M. V. Twigg, J. Organometal. Chem., 67, C75 (1974).
4. M. I. Bruce, G. Shaw, and F. G. A. Stone, J. Chem. Soc., Dalton, 2094 (1972).
5. J. P. Candlin and A. C. Shortland, J. Organometal. Chem., 16, 289 (1969).
6. D. B. W. Yawney and F. G. A. Stone, J. Chem. Soc. (A), 502 (1969).
7. U. Anders and W. A. G. Graham, Chem. Commun., 291 (1966).
8. E. H. Schubert and R. K. Sheline, Z. Naturforsch., 20B, 1306 (1965).
9. G. O. Evans and R. K. Sheline, J. Inorg. Nucl. Chem., 30, 2862 (1968).
10. G. O. Evans, J. P. Hargaden, and R. K. Sheline, Chem. Commun., 186 (1967).
11. R. K. Sheline and K. S. Pitzer, J. Am. Chem. Soc., 72, 1107 (1950).
12. R. A. Levenson, H. B. Gray, and G. P. Ceasar, J. Am. Chem. Soc., 92, 3653 (1970).
13. L. F. Dahl and R. E. Rundle, J. Chem. Phys., 27, 323 (1957).

14. N. A. Beach and H. B. Gray, J. Am. Chem. Soc., 90, 5713 (1968).

15. R. Mason and A. I. M. Rae, J. Chem. Soc. (A), 778 (1968). A redetermination of the $Ru_3(CO)_{12}$ structure was reported recently. See M. R. Churchill, F. J. Hollander, and J. P. Hutchinson, Inorg. Chem., 16, 2655 (1977). The small differences in reported bond angles and bond lengths should not affect the results significantly.

16. B. J. Ransil, Rev. Mod. Phys., 32, 245 (1960).

17. H. Basch and H. B. Gray, Theoret. Chim. Acta, 4, 367 (1966).

18. A complete listing of eigenvalues and eigenvectors for $Ru(CO)_4$ and $Ru_3(CO)_{12}$ is available. See paragraph at end of paper regarding supplementary material.

19. M. Elian and R. Hoffman, Inorg. Chem., 14, 1058 (1975).

20. E. R. Corey, Ph.D. Thesis, University of Wisconsin, 1963.

21. (a) A. J. Deeming, B. F. G. Johnson, and J. Lewis, J. Chem. Soc. (A), 897 (1970); (b) M. I. Bruce, G. Shaw, and F. G. A. Stone, J. Chem. Soc., Dalton, 2094 (1972).

22. C. O. Quicksall and T. G. Spiro, Inorg. Chem., 7, 2365 (1968).

23. H. B. Abrahamson, C. C. Frazier, D. S. Ginley, H. B. Gray, J. Lilienthal, D. R. Tyler, and M. S. Wrighton, Inorg. Chem., 16, 1554 (1977).

24. M. Dartiguenave, Y. Dartiguenave, and H. B. Gray, Bull. Soc. Chim. Fr., 4223 (1969).

25. P. A. Agron, R. D. Ellison, and H. A. Levy, Acta Cryst., 23, 1079 (1967).

26. L. F. Dahl and R. E. Rundle, Acta Cryst., 16, 491 (1963).

27. D. R. Tyler and H. B. Gray, unpublished results.

CHAPTER 2

The Photochemistry of $Os_3(CO)_{12}$

Abstract: $Os_3(CO)_{12}$ reacts photochemically with CCl_4, $CHCl_3$, or CH_2Cl_2 at room temperature to give $Os(CO)_4Cl_2$. No spectroscopic evidence was obtained for the intermediate formation of either $Os_3(CO)_{12}Cl_2$ or $Os_2(CO)_8Cl_2$. The quantum yields for these reactions are very low: 0.002 for the reaction with CCl_4 at 313 nm. We suggest that $Os_3(CO)_{12}Cl_2$ might not be observed because it is so photoreactive. This molecule reacts photochemically with CCl_4 to give $Os(CO)_4Cl_2$ with a quantum yield of 0.31 at 313 nm. Substitution of $Os_3(CO)_{12}$ appears to be a much more efficient photoprocess than fragmentation. $Os_3(CO)_{12}$ reacts photochemically with PPh_3 at room temperature to give $Os_3(CO)_{11}PPh_3$. $Os_3(CO)_{10}(PPh_3)_2$ and $Os_3(CO)_9(PPh_3)_3$ are secondary and tertiary photolysis products. The trisubstituted complex reacts slowly with PPh_3 to yield $Os(CO)_3(PPh_3)_2$ (Φ = 0.005 at 366 nm). The photochemistry of $Os_3(CO)_{12}$ is remarkably different from that of $Ru_3(CO)_{12}$ because photochemical fragmentation is much more efficient in the latter. We believe this can be ascribed to the different natures of the lowest energy electronic excited states of the two compounds. In $Ru_3(CO)_{12}$, the lowest excited state is $\sigma \rightarrow \sigma^*$ (metal-metal bonding to metal-metal antibonding). Such a state should certainly lead to metal-metal bond cleavage and fragmentation. In $Os_3(CO)_{12}$, the lowest excited state is $\sigma^{*\prime} \rightarrow \sigma^*$ (metal-metal antibonding to metal-metal antibonding). This state will not necessarily lead to efficient metal-metal bond cleavage. The result is that Os-CO dissociation is more efficient than fragmentation.

Johnson, Lewis, and Twigg have reported the photofragmentation of the $Ru_3(CO)_{12}$ molecule (1,2). The mechanism of the fragmentation of this cluster and of other trinuclear clusters is a problem of interest to photochemists. It has been assumed, but never shown, that absorption of a photon initially cleaves one metal-metal bond to give a "diradical" excited state(3). Other pathways are

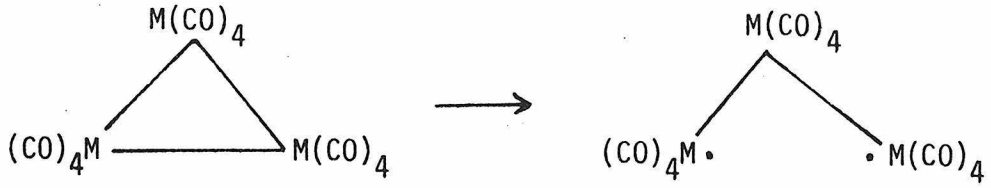

possible, however. For instance, the concerted cleavage of two metal-metal bonds to eliminate a $M(CO)_4$ fragment from the triangular cluster is energetically feasible with near-uv radiation. Or, perhaps cleavage of all the metal-metal bonds occurs simultaneously to yield three $Ru(CO)_4$ fragments.

$Ru_3(CO)_{12}$ is not the best $M_3(CO)_{12}$ cluster with which to study the photofragmentation mechanism; rather, $Os_3(CO)_{12}$ is. The reason for this is that it is possible to trap the fragments formed in the photolysis of $Os_3(CO)_{12}$ as stable molecules. For example, the diradical mentioned above can react with a chlorocarbon solvent to give $Os_3(CO)_{12}Cl_2$ (4). Similarly, the dimer formed by the elimination of $Os(CO)_4$ would give $Os_2(CO)_8Cl_2$ (4). Both of these osmium chloride complexes are known and stable molecules. However, the

isoelectronic Ru complexes are unknown (4). For this reason, we decided to study the mechanism of the photofragmentation of the triangular clusters by studying the $Os_3(CO)_{12}$ complex. Herein we report the results of our study.

Experimental

$Os_3(CO)_{12}$ was purchased from Strem Chemical Company. $Os_3(CO)_{12}Cl_2$ (5) and $Os(CO)_4Cl_2$ (6) were synthesized by standard literature methods. When necessary for comparison purposes, the phosphine substituted derivatives of $Os_3(CO)_{12}$ were prepared by the method of Deeming, Johnson, and Lewis (7). Triphenylphosphine (PPh_3) was purchased from MCB Chemical Company. Triethylphosphine was purchased from Strem Chemical Company. Spectroquality solvents were purchased from MCB Chemical Company and were dried by standard procedures (8).

Electronic absorption spectra and spectral changes were recorded with a Cary 17 spectrophotometer. Infrared spectra were recorded with a Perkin-Elmer 225 instrument or a Beckman IR-12 instrument. A 1000 watt high pressure Hg-Xe arc lamp in conjuction with Corning cut-off filters was used for the irradiations. Low pressure Hg lamps were used for the 254 nm irradiations.

Ferrioxalate actiometry was used for quantum yield determinations at 254, 311, and 366 nm (9). The procedure was modified to adopt the precautions recently suggested by Bowman and Demas (10). The quantum yields for the reactions of $Os_3(CO)_{12}$ with chlorocarbon solvents

were determined by monitoring the disappearance of the 300 nm band of $Os_3(CO)_{12}$. Similarly, the quantum yield for the reaction of $Os_3(CO)_9(PPh_3)_3$ with PPh_3 was determined by monitoring the disappearance of the band at 422 nm in $Os_3(CO)_9(PPh_3)_3$.

Photolyses were done in special two-arm evacuable cells equipped with Kontes quick-release valves. One arm is a glass bulb and the other is a quartz spectrophotometer cell. Photolysis solutions in the glass bulb were degassed by four freeze-pump-thaw cycles. The electronic spectrum of the solution is measured by transferring the solution into the quartz cell. Thick-walled quartz or glass cells equipped with Kontes quick-release valves were used for the photolyses done under CO pressure. Pressures up to six atmospheres were obtainable in these cells. In a typical experiment, a 10^{-4} M solution of $Os_3(CO)_{12}$ or one of its derivatives was irradiated. Phosphine-substitution experiments were done in the presence of a ten-fold excess of the phosphine, i.e. $[PR_3] \simeq 10^{-3}$ M. Typical photon fluxes into the photochemical cell were 6×10^{-7}, 2×10^{-7}, and 1×10^{-7} einsteins per minute at 254, 313, and 366 nm, respectively.

Results

Photolysis of a CCl_4 solution of $Os_3(CO)_{12}$ ($\simeq 10^{-4}$ M) at room temperature results in the disappearance of the $Os_3(CO)_{12}$ and appearance of a product with IR stretches at 2054, 2094, 2120, and 2187 cm^{-1} in

the CO stretching region. This product was identified as $Os(CO)_4Cl_2$ by comparison with the infrared spectrum reported by L'Eplattenier and Calderazzo (6). We studied the wavelength dependence of the $Os_3(CO)_{12}$ photolysis and found that the same product, $Os(CO)_4Cl_2$, formed at 254, 313, 366, and 405 nm. $Os(CO)_4Cl_2$ also formed when the chlorocarbon solvent was $CHCl_3$ or CH_2Cl_2. Quantum yields for the reaction at various wavelengths in CCl_4, $CHCl_3$, and CH_2Cl_2 are shown in Table 1. In none of the photolyses of $Os_3(CO)_{12}$ were we able to see any infrared or uv-visible spectroscopic evidence for $Os_3(CO)_{12}Cl_2$ or $Os_2(CO)_8Cl_2$ (4, 11).

Prolonged photolysis of $Os_3(CO)_{12}$ in the chlorocarbon solvents gave an additional product with infrared CO stretching bands at 2134 and 2061 cm^{-1}. This product is $(Os(CO)_3Cl_2)_2$, identified by comparison to the literature infrared spectrum (12). We suspected that $(Os(CO)_3Cl_2)_2$ was a secondary product formed by the photolysis of $Os(CO)_4Cl_2$. Indeed, when a CCl_4 solution of pure $Os(CO)_4Cl_2$ was photolyzed at 313 nm the product was $(Os(CO)_3Cl_2)_2$.

The electronic absorption spectrum of $Os_3(CO)_{12}Cl_2$ is reported in Table 2. This complex has an absorption band at 348 nm with an extinction coefficient of 19,500. This absorption band overlaps with the lowest energy absorption bands of $Os_3(CO)_{12}$ into which we were irradiating (Table 2 and Figure 1). Thus, it is possible that $Os_3(CO)_{12}Cl_2$is not observed in the photolysis of $Os_3(CO)_{12}$ with the chlorocarbon solvents because $Os_3(CO)_{12}Cl_2$ can react

Table 1. Quantum yields for the Reaction of $Os_3(CO)_{12}$ with Chlorocarbon Solvents to give $Os(CO)_4Cl_2$. The quantum yields were measured for the disappearance of $Os_3(CO)_{12}$.

Solvent	Wavelength	
	313 nm	254 nm
CCl_4	0.002	0.01
$CHCl_3$	0.002	0.006
CH_2Cl_2	0.0004	0.002

Table 2. Spectral Data for the $\sigma \rightarrow \sigma^*$ and $\sigma^{*\prime} \rightarrow \sigma^*$ Electronic Absorption Bands in $Os_3(CO)_{12}$ and Several Derivatives.[a]

Complex	λ_{max} (nm)	$\bar{\nu}_{max}$ (μm^{-1})	$\varepsilon_M \times 10^{-3}$
$Os_3(CO)_{12}$[b]	385 sh	2.60	3.6
	330	3.03	8.6
$Os_3(CO)_{11}PPh_3$	408	2.45	
	345	2.90	
$Os_3(CO)_{10}(PPh_3)_2$	427	2.34	
	355	2.82	
$Os_3(CO)_9(PPh_3)_3$	422	2.37	7.2
	347	2.88	9.4
$Os_3(CO)_{11}PEt_3$	407	2.46	
	340	2.94	
$Os_3(CO)_{10}(PEt_3)_2$	427	2.34	
	355	2.82	
$Os_3(CO)_9(PEt_3)_3$	440	2.27	
	375	2.67	
$Os_3(CO)_{12}Cl_2$[c]	348	2.87	19.5

[a] In toluene unless otherwise noted.

[b] In 2-methypentane.

[c] In CCl_4.

photochemically with chlorocarbon solvents. To check this possibility, we photolyzed (366 and 313 nm) a CCl_4 solution of $Os_3(CO)_{12}Cl_2$. An infrared spectrum of the photolyzed solution showed that $Os(CO)_4Cl_2$ was the product (6). The reaction is relatively efficient; the quantum yields for the disappearance of $Os_3(CO)_{12}Cl_2$ at 366 and 313 nm are 0.16 and 0.31, respectively. Once again, the infrared spectrum of the products showed no evidence for $Os_2(CO)_8Cl_2$ (11) or any products other than $Os(CO)_4Cl_2$.

It was clear, at this point, that attempts to trap the primary fragmentation products of $Os_3(CO)_{12}$ with chlorocarbon solvents were futile. However, there are other ways to trap these fragments. For instance, if a $Os(CO)_4$ fragment is extruded from the $Os_3(CO)_{12}$ triangle, leaving behind the $Os_2(CO)_8$ species, then perhaps CO will trap these fragments to give $Os(CO)_5$ (13) and $Os_2(CO)_9$ (14). Complete fragmentation of the $Os_3(CO)_{12}$ cluster would yield three $Os(CO)_5$ molecules.

Irradiation for two hours at 254, 313, and 366 nm of an acetonitrile solution of $Os_3(CO)_{12}$ under six atmospheres of CO resulted in no net photolysis. The photoreaction of $Os(CO)_5$ to give $Os_3(CO)_{12}$ is well known (13) so to avoid this reaction we also photolyzed the $Os_3(CO)_{12}$ solutions at wavelengths greater than 410 nm ($\lambda > 410$ nm), wavelengths at which $Os(CO)_5$ does not absorb. Even under these conditions, there was no disappearance of $Os_3(CO)_{12}$ from the solution.

Figure 1

The electronic spectra of $Os_3(CO)_{12}$ (A) and $Os_3(CO)_{12}Cl_2$ (B) in CCl_4.

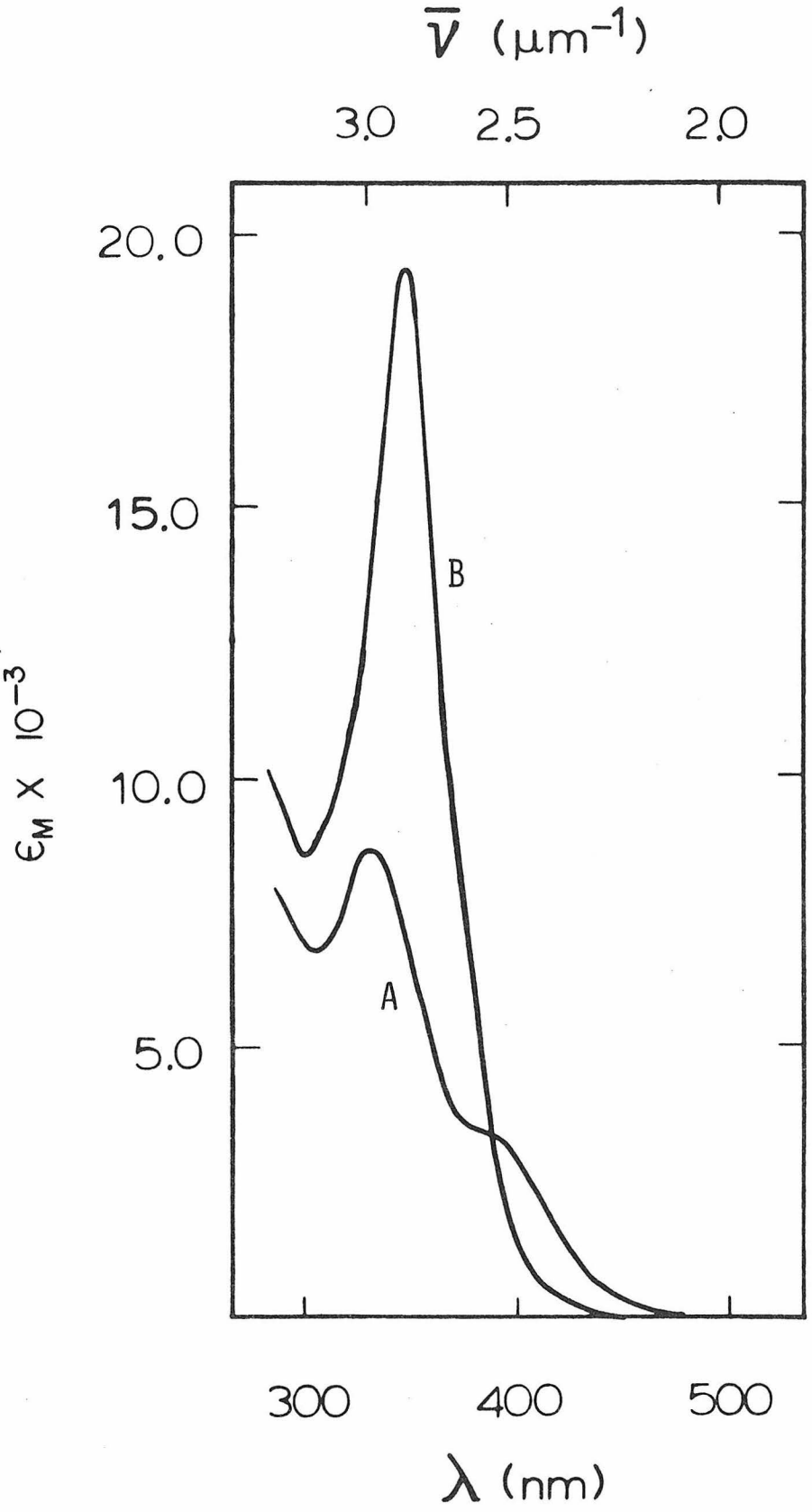
$\bar{\nu}$ (μm^{-1})
3.0
2.5
2.0
20.0
15.0
10.0
5.0
$\epsilon_M \times 10^{-3}$
B
A
300
400
500
λ (nm)

Irradiation of $Os_3(CO)_{12}$ with phosphines also did not yield any primary fragmentation products. For example, irradiation of a toluene solution of $Os_3(CO)_{12}$ (10^{-4} M) with PPh_3 (10^{-3} M) at 366 nm gave a mixture of $Os_3(CO)_{11}(PPh_3)$, $Os_3(CO)_{10}(PPh_3)_2$, and $Os_3(CO)_9(PPh_3)_3$. These complexes were identified as reaction products by comparison of the infrared spectra of the products to the infrared spectra of the substituted complexes reported by Tripathi, Srivastava, Mani, and Shrimal (4). By monitoring the photoreaction with infrared spectroscopy, we found that the phosphines substituted stepwise. That is, short irradiation times yielded mainly $Os_3(CO)_{11}(PPh_3)$. The disubstituted complex built up with longer irradiation periods and still longer irradiation times yielded the trisubstituted complex. Other chemical evidence suggests that the substitution of PPh_3 is stepwise. Photolysis ($\lambda > 320$ nm) of toluene solution of $Os_3(CO)_{11}(PPh_3)$ with PPh_3 initially yields $Os_3(CO)_{10}(PPh_3)_2$ while $Os_3(CO)_9(PPh_3)_3$ formed upon prolonged photolysis. Similarly photolysis ($\lambda > 320$ nm) of $Os_3(CO)_{10}(PPh_3)_2$ with excess PPh_3 gave $Os_3(CO)_9(PPh_3)_3$.

Exhaustive photolysis of the $Os_3(CO)_{12}$-PPh_3 solutions above caused the $Os_3(CO)_9(PPh_3)_3$ to disappear and a precipitate to form. The precipitate readily dissolves in CCl_4 and an infrared spectrum (1890 cm^{-1}) shows it to be $Os(CO)_3(PPh_3)_2$ (15). This is the product expected if the trisubstituted complex, $Os_3(CO)_9(PPh_3)_3$, photolytically fragmented to three $Os(CO)_3(PPh_3)$ species. These coordinately unsaturated fragments would then be scavenged by

PPh_3 to give the stable $Os(CO)_3(PPh_3)_2$ complex:

$$Os_3(CO)_9(PPh_3)_3 \xrightarrow{h\nu} 3\ Os(CO)_3(PPh_3) \xrightarrow{3\ PPh_3} 3\ Os\ (CO)_3(PPh_3)_2.$$

To verify this, we photolyzed a thermally produced sample of $Os_3(CO)_9(PPh_3)_3$ in toluene with excess PPh_3. The product is indeed $Os(CO)_3(PPh_3)_2$. The quantum yield for this reaction is 0.005 at 366 nm.

None of the infrared spectra of the $Os_3(CO)_{12}$-PPh_3 photolysis solutions had bands attributable to $Os(CO)_4PPh_3$ (15) which is the expected product if initial fragmentation of $Os_3(CO)_{12}$ occurred:

$$Os_3(CO)_{12} \xrightarrow{h\nu} 3\ Os(CO)_4 \xrightarrow{3\ PPh_3} 3\ Os(CO)_4PPh_3.$$

Of course, $Os(CO)_4PPh_3$ might be reacting photochemically with the excess PPh_3 to give the $Os(CO)_3PPh_3)_2$. This is doubtful. $Os(CO)_4PPh_3$ is a colorless compound; it has no absorption bands or tails in the visible region (15). $Os(CO)_3(PPh_3)_2$ forms even when $Os_3(CO)_{12}$ and PPh_3 are irradiated at wavelengths as long as 420 nm. A photoreaction of $Os(CO)_4PPh_3$ is not possible because the molecule does not absorb at these wavelengths.

Results similar to those obtained above are obtained if trimethylphosphite and tri-n-butylphosphine are used instead of PPh_3.

As explained more fully below, we were unable to measure the absolute quantum yields for the reactions of $Os_3(CO)_{12}$ with phosphines. However, we could determine relative quantum yields with

a uv-vis spectrophotometer by measuring the extent of the reaction after a constant period of irradiation. In this fashion we were able to determine that the disappearance quantum yield at 366 nm for the photoreaction of $Os_3(CO)_{12}$ ($\simeq 10^{-4}$ M) with tri-n-butylphosphine is independent of the phosphine concentration for phosphine concentrations in the range 10^{-2} - 10^{0} M.

Discussion

Electronic Spectra

We have discussed the electronic structure of $Os_3(CO)_{12}$ in a previous paper (16). The lowest energy features of the electronic spectrum are a band at 328 nm and a shoulder on this band at 390 nm. Based on a molecular orbital calculation and the MCD spectrum of the complex, we assigned the band at 328 nm to a metal-metal bonding to antibonding transition ($\sigma \rightarrow \sigma^*$) and the shoulder at 390 nm to a metal-metal antibonding to antibonding transition ($\sigma^{*\prime} \rightarrow \sigma^*$).

The phosphine-substituted $Os_3(CO)_{12}$ complexes are similar to $Os_3(CO)_{12}$ in having two transitions in the near-uv region of the spectrum (Table 2). Based on simple ligand field arguments, we predicted and showed that phosphine substitution of $Ru_3(CO)_{12}$ should increase the energy separation of the $\sigma \rightarrow \sigma^*$ and $\sigma^{*\prime} \rightarrow \sigma^*$ transitions (16). The same ligand field arguments apply to $Os_3(CO)_{12}$ as well as to $Ru_3(CO)_{12}$ and, therefore, a similar effect should also be observed for substituted $Os_3(CO)_{12}$ complexes. Indeed, Table 2 shows that successive triphenylphosphine substitution

successively increases the energy separation of the two lowest energy bands. Because of this and because of the similarity of the spectra of the phosphine-substituted complexes to the spectrum of $Os_3(CO)_{12}$ in general, we assign the two lowest energy bands in the substituted complexes to the $\sigma \rightarrow \sigma^*$ and $\sigma^{*\prime} \rightarrow \sigma^*$ transitions. As in $Os_3(CO)_{12}$, we assign the lowest energy band to the $\sigma^{*\prime} \rightarrow \sigma^*$ transition and the higher energy band to the $\sigma \rightarrow \sigma^*$ transition. Note that the $\sigma \rightarrow \sigma^*$ band also shifts to slightly lower energies upon phosphine substitution. This effect has been observed in other polynuclear metal carbonyl complexes (17). The spectra of the triethylphosphine substituted $Os_3(CO)_{12}$ complexes are also reported in Table 2.

Photochemistry

The results of the photochemical reactions of $Os_3(CO)_{12}$ with chlorocarbon solvents are summarized in Figure 2. Note that the quantum yield for the reaction of $Os_3(CO)_{12}Cl_2$ with CCl_4 is 0.31 (313 nm) while the overall quantum yield for the disappearance of $Os_3(CO)_{12}$ in CCl_4 at 313 nm is 0.002. Thus, it is clear that $Os_3(CO)_{12}Cl_2$, if formed in the reaction of $Os_3(CO)_{12}$ with CCl_4, will never build up in sufficient concentrations to be observed spectroscopically because it is too photoreactive. Also note that the overlapping absorption bands of $Os_3(CO)_{12}$ and $Os_3(CO)_{12}Cl_2$ (Table 2) preclude irradiation of just $Os_3(CO)_{12}$ in an attempt to

Figure 2

The photochemical reactions of $Os_3(CO)_{12}$ with chlorocarbon solvents.

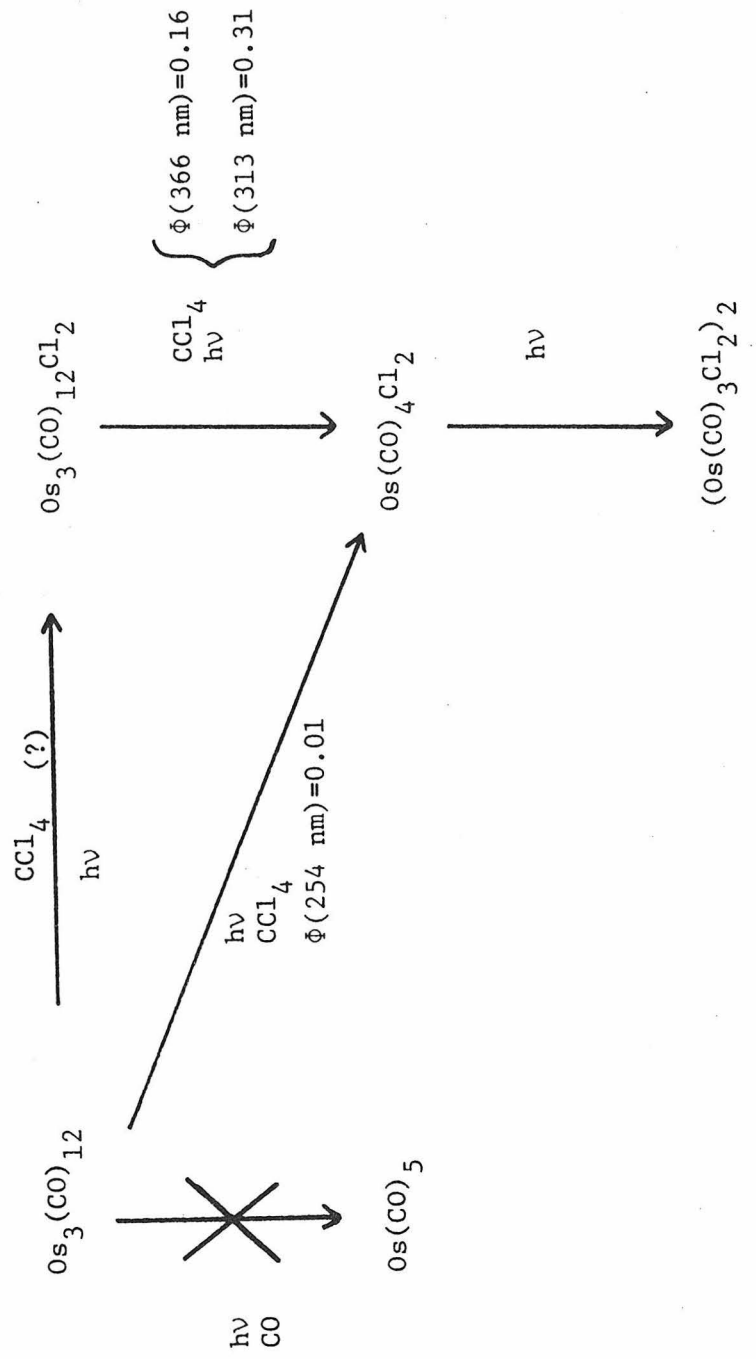
$Os_3(CO)_{12}$
$Os_3(CO)_{12}Cl_2$
CCl_4 (?)
$h\nu$
CCl_4
$h\nu$
Φ(366 nm)=0.16
Φ(313 nm)=0.31
$h\nu$
CO
$Os(CO)_5$
$h\nu$
CCl_4
Φ(254 nm)=0.01
$Os(CO)_4Cl_2$
$h\nu$
$(Os(CO)_3Cl_2)_2$

build up the $Os_3(CO)_{12}Cl_2$ concentration. Because we are unable to spectroscopically observe any $Os_3(CO)_{12}Cl_2$ or $Os_2(CO)_8Cl_2$ we conclude that the reactions of $Os_3(CO)_{12}$ with chlorocarbon solvents cannot be used to elucidate the photochemical fragmentation mechanism of the $M_3(CO)_{12}$ complexes.

The results of the photochemical PPh_3 substitution reactions of $Os_3(CO)_{12}$ are summarized in Figure 3. The point which needs to be emphasized is that fragmentation of the cluster does not occur in the reaction of $Os_3(CO)_{12}$ with phosphines. Rather, the substituted cluster complex, $Os_3(CO)_{11}PPh_3$ forms. Only after each Os atom has been substituted once will the cluster undergo fragmentation. As in the fragmentation reactions of $Os_3(CO)_{12}$ with chlorocarbon solvents, the photofragmentation of the $Os_3(CO)_9(PPh_3)_3$ cluster is inefficient. The disappearance quantum yield for the reaction of $Os_3(CO)_9(PPh_3)_3$ with PPh_3 is ≤ 0.005 at 366 nm.

We were unable to measure the quantum yields for the phosphine substitution reactions of $Os_3(CO)_{12}$ and $Os_3(CO)_{12-x}(PPh_3)_x$ ($x = 1,2$) because of the overlapping absorption bands of the reactants and products. Qualitatively, we noted that the substitution reactions were much faster than the fragmentation reaction of $Os_3(CO)_9(PPh_3)_3$. For example, total conversion of $Os_3(CO)_{12}$ to $Os_3(CO)_9(PPh_3)_3$ ($\lambda > 320$ nm) took place in 30 minutes. Continued irradiation of the $Os_3(CO)_9(PPh_3)_3$ solution to produce $Os(CO)_3(PPh_3)_2$ took three more hours. The conclusion we draw from this result is that Os-CO

Figure 3

The photochemical reactions of $Os_3(CO)_{12}$ with PPh_3.

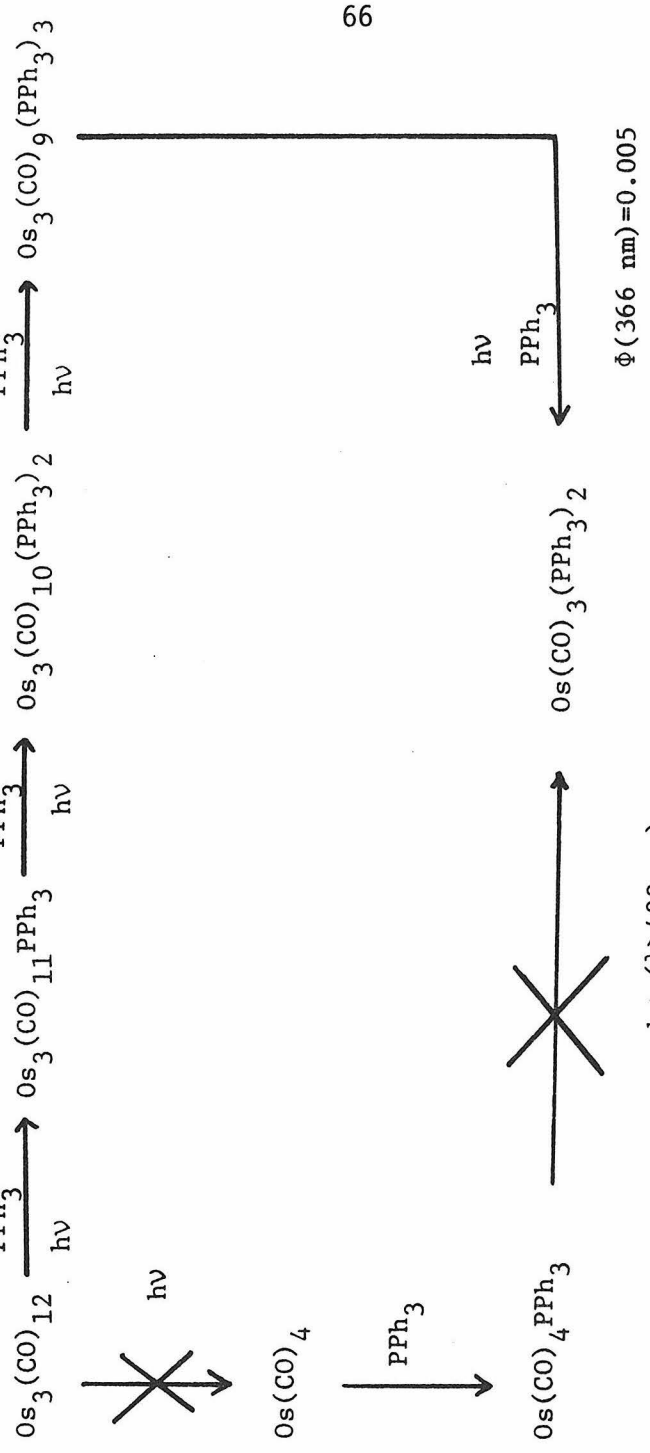
Os3(CO)12
PPh3
hν
Os3(CO)11PPh3
PPh3
hν
Os3(CO)10(PPh3)2
PPh3
hν
Os3(CO)9(PPh3)3
hν
Os(CO)4
PPh3
Os(CO)4PPh3
hν (λ>420 nm)
PPh3
Os(CO)3(PPh3)2
hν
PPh3
Φ(366 nm)=0.005

dissociation is a much more efficient photochemical process than cleavage of the Os-Os bonds.

Johnson, Lewis, and Twigg found the same two photochemical processes, fragmentation and M-CO dissociation, in their study of the $Ru_3(CO)_{12}$ molecule (1,2). However, they found that cleavage of the metal-metal bonds was an efficient photoprocess in $Ru_3(CO)_{12}$, unlike in $Os_3(CO)_{12}$. They also found that cleavage of the Ru-Ru bonds was an efficient process in the phosphine substituted cluster. So efficient, in fact, that $Ru_3(CO)_{10}(PPh_3)_2$ and $Ru_3(CO)_9(PPh_3)_3$ never form in the photoreaction of $Ru_3(CO)_{12}$ with PPh_3 because photochemical fragmentation of $Ru_3(CO)_{11}PPh_3$ is so efficient. The point here is that photochemical cleavage of the metal-metal bonds is more efficient than Ru-CO dissociation while in $Os_3(CO)_{12}$ the relative efficiencies of the two pathways are reversed.

Consistent with the idea that Os-CO dissociation is the preferred photochemical pathway is the lack of reaction between $Os_3(CO)_{12}$ and CO. Obviously, $Os_3(CO)_{12}$ can react with CO to give a net reaction only by a fragmentation pathway (i.e., to give $Os(CO)_5$ or $Os_2(CO)_9$). Irradiation of an $Os_3(CO)_{12}$ solution under six atmospheres of CO for several hours (λ = 254, 313, and 366 nm) produced no change in the concentration of $Os_3(CO)_{12}$. This points out the low quantum efficiency of the fragmentation pathway.

The reason for the different photochemical behavior of $Ru_3(CO)_{12}$ and $Os_3(CO)_{12}$ is not simply due to the expected increase

in the Os-Os bond strength as compared to the Ru-Ru bond strength (18). We feel, rather, that the difference is caused by the dissimilar natures of the lowest excited states of the two compounds. In $Ru_3(CO)_{12}$ the lowest energy transition is $\sigma \rightarrow \sigma^*$ (16). Depopulation of a metal-metal bonding orbital and population of a metal-metal antibonding orbital should certainly weaken a Ru-Ru bond. Thus, fragmentation is an efficient process in $Ru_3(CO)_{12}$. As discussed earlier, the lowest excited states of $Os_3(CO)_{12}$ and $Os_3(CO)_{12-x}(PPh_3)_x$ (x = 1-3) are $\sigma^{*\prime} \rightarrow \sigma^*$. Although once again the σ^* (metal-metal antibonding) orbital is being occupied, the orbital being depopulated is also metal-metal antibonding. Such an excited state will not necessarily lead to metal-metal bond cleavage. However, the excited state apparently has enough M-CO antibonding character such that M-CO dissociation is the preferred pathway. Of course, our argument assumes that internal conversion from the higher energy $\sigma \rightarrow \sigma^*$ excited state to the $\sigma^{*\prime} \rightarrow \sigma^*$ state is rapid. Otherwise, irradiation in the $\sigma \rightarrow \sigma^*$ band would yield fragmentation products and irradiation in the $\sigma^{*\prime} \rightarrow \sigma^*$ band would yield substitution products. As the quantum yields in Table 1 show, fragmentation is still very inefficient at 313 nm. From this we conclude that the photoactive state in $Os_3(CO)_{12}$ is the lowest excited state, $\sigma^{*\prime} \rightarrow \sigma^*$.

Yet another substitution pathway would involve initial formation of the diradical, followed by PPh_3 substitution for CO at one of the 17-electron Os atoms (19), followed by reformation of

the Os-Os bond (Figure 4). This mechanism has been proposed for phosphine substitution in $HCCo_3(CO)_9$ (20). However, we feel this substitution mechanism is less likely than the direct Os-CO dissociation mechanism proposed above for several reasons. First, this mechanism requires the initial cleavage of an Os-Os bond. As discussed above, excitation to the $\sigma^{*\prime} \rightarrow \sigma^*$ excited state should not necessarily cleave a metal-metal bond. Second, Kidd and Brown have pointed out that 17-electron metal fragments are extremely labile (19). Substitution in such fragments occurs at a rate much faster than the rate of recombination of two fragments to form a metal-metal bond. Thus, a disubstituted phosphine complex would be the initial product if $Os_3(CO)_{12}$ underwent substitution via a "diradical" intermediate. Finally, we note that $HCCo_3(CO)_9$ has a face-bridging CH group (20) while $Os_3(CO)_{12}$ has no metal-metal bond-bridging ligands. We have recently shown that cluster complexes with bridging ligands do not fragment as easily as those without bridging ligands (21). Thus, while $HCCo_3(CO)_9$ may be able to undergo cleavage of one metal-metal bond and subsequent phosphine substitution without fragmenting, the $Os_3(CO)_{12}$ diradical intermediate will certainly fragment some of the time. In such a case we would expect to see some $Os(CO)_4PPh_3$:

$$Os_3(CO)_{12} \xrightarrow{h\nu} 3\ Os(CO)_4 \xrightarrow{3\ PPh_3} 3\ Os(CO)_4PPh_3.$$

Figure 4

An alternative photosubstitution mechanism of $Os_3(CO)_{12}$ involving a diradical intermediate.

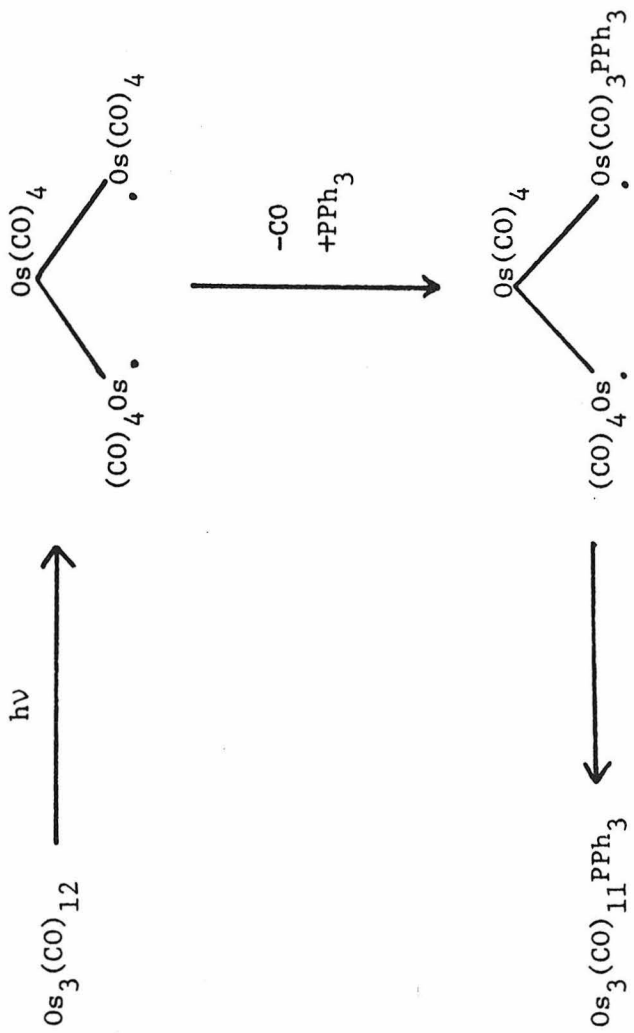
$Os_3(CO)_{12}$
hν
$(CO)_4Os$
$Os(CO)_4$
$Os(CO)_4$
-CO
$+PPh_3$
$(CO)_4Os$
$Os(CO)_4$
$Os(CO)_3PPh_3$
$Os_3(CO)_{11}PPh_3$

Recall that no $Os(CO)_4PPh_3$ was observed spectroscopically, which implies that the diradical is not involved in the substitution process.

References

1. B. F. G. Johnson, J. Lewis, and M. V. Twigg, J. Organometal. Chem., 67, C75 (1974).
2. B. F. G. Johnson, J. Lewis, and M. V. Twigg, J. Chem. Soc., Dalton Trans., 1876 (1975).
3. M. S. Wrighton, Topics Current Chem., 65, 68 (1977).
4. S. C. Tripathi, S. C. Srivastava, R. P. Mani, and A. K. Shrimal, Inorg. Chim. Acta, 15, 249 (1975).
5. B. F. G. Johnson, J. Lewis, and P. A. Kitty, J. Chem. Soc.,(A), 2859 (1968).
6. F. L' Eplattenier and F. Calderazzo, Inorg. Chem., 6, 2092 (1967).
7. A. J. Deeming, B. F. G. Johnson, and J. Lewis, J. Chem. Soc., (A), 897 (1970).
8. D. D. Perrin, W. L. F. Armarego, and D. R. Perrin, Purification of Laboratory Chemicals, Pergamon Press, London (1966).
9. J. G. Calvert and J. N. Pitts, Photochemistry, John Wiley and Sons, Inc., New York, N.Y. (1966).
10. W. D. Bowman and J. N. Demas, J. Phys. Chem., 80, 2434 (1976).
11. J. R. Moss and W. A. G. Graham, J. Chem. Soc., Dalton Trans., 89 (1977).
12. L. A. W. Hales and R. J. Irving, J. Chem. Soc., (A), 1932 (1967).
13. F. Calderazzo and F. L' Eplattenier, Inorg. Chem., 6, 1220 (1967).
14. J. R. Moss and W. A. G. Graham, J. Chem. Soc., Dalton Trans, 95 (1977).

15. F. L' Eplattenier and F. Calderazzo, Inorg. Chem., 7, 1290 (1968).

16. D. R. Tyler, R. A. Levenson, and H. B. Gray, J. Am. Chem. Soc., in press.

17. R. A. Levenson and H. B. Gray, J. Am. Chem. Soc., 97, 6042 (1975).

18. C. O. Quicksall and T. G. Spiro, Inorg. Chem., 7, 2365 (1968).

19. D. L. Kidd and T. L. Brown, J. Am. Chem. Soc., 100, 4095 (1978).

20. G. L. Geoffroy and R. A. Epstein, Inorg. Chem., 16, 2795 (1977).

21. D. R. Tyler and H. B. Gray, unpublished results.

CHAPTER 3

The Photochemistry of $Fe_3(CO)_{11}^{2-}$

Abstract: Irradiation (λ < 313 nm) of 1 M NaOH solutions of $Fe_3(CO)_{11}^{2-}$ yields $Fe(CO)_4^{2-}$ + $2Fe(OH)_2$ + 7CO + $2H_2$. Studies in non-aqueous solvents show that the photofragmentation of $Fe_3(CO)_{11}^{2-}$ is inhibited in the presence of excess CO. Therefore, it is proposed that the fragmentation occurs by the following pathway: (1) $Fe_3(CO)_{11}^{2-} \rightleftarrows Fe_3(CO)_{10}^{2-}$ + CO (2) $Fe_3(CO)_{10}^{2-} \rightarrow Fe(CO)_4^{2-}$ + $2Fe(CO)_3$. Evidence for the formation of two moles of $Fe(CO)_3$ comes from the photolysis of $Fe_3(CO)_{11}^{2-}$ in acetonitrile solution with excess triphenylphosphine: $Fe_3(CO)_{11}^{2-}$ + $2PPh_3 \rightarrow Fe(CO)_4^{2-}$ + $2Fe(CO)_3(PPh_3)_2$ + CO. Under these conditions an $Fe(CO)_3$ fragment reacts with PPh_3 to form the stable $Fe(CO)_3(PPh_3)_2$ molecule. The formation of two $Fe(CO)_3$ fragments is also consistent with the photolyses done in 1 M NaOH. In this case, the two $Fe(CO)_3$ fragments are oxidized to Fe(II), the reduction product being two moles of H_2. Photochemical excitation of triangular cluster molecules is thought to produce an excited state with one metal-metal bond broken, a "diradical." In the case of $Fe_3(CO)_{11}^{2-}$ it is proposed that the face-bridging CO ligands in $Fe_3(CO)_{11}^{2-}$ prevent structural distortion of this excited state thereby facilitating reformation of the metal-metal bond and preventing fragmentation of the cluster by further metal-metal bond cleavage. The photochemistry which is observed occurs by dissociation of CO from this excited state diradical but can also result directly from excitation into higher energy MLCT states.

In 1962, Hieber and Schubert reported the aqueous solution photochemistry of the $HFe(CO)_4^-$ and $Fe_2(CO)_8^{2-}$ anions (1). The results of their study are summarized in equations (1) and (2).

$$2HFe(CO)_4^- \xrightarrow{uv} H_2 + Fe_2(CO)_8^{2-} \quad (1)$$

$$2Fe_2(CO)_8^{2-} \xrightarrow{uv} Fe(CO)_4^{2-} + Fe_3(CO)_{11}^{2-} + CO \quad (2)$$

Recently, Johnson, Lewis, and Twigg (2) have shown that certain polynuclear metal carbonyl clusters can be photofragmented to monomeric metal carbonyl complexes. Equation (3) is an example of this type of photoreaction.

$$Ru_3(CO)_{12} + 3CO \xrightarrow{h\nu} Ru(CO)_5 \quad (3)$$

Presumably, irradiation induces homolytic bond cleavage to give three $Ru(CO)_4$ fragments, which are then trapped by CO. The idea occurred to us that perhaps the trinuclear product in Hieber's reactions, $Fe_3(CO)_{11}^{2-}$, could also be photofragmented, as in reaction (4).

$$Fe_3(CO)_{11}^{2-} \xrightarrow{h\nu} Fe(CO)_4^{2-} + Fe(CO)_3 + Fe(CO)_4 \quad (4)$$

The unstable $Fe(CO)_3$ and $Fe(CO)_4$ fragments generated in this reaction could be scavenged by CO to give $Fe(CO)_5$.

$$Fe(CO)_4 + CO \rightarrow Fe(CO)_5 \quad (5)$$

$$Fe(CO)_3 + 2CO \rightarrow Fe(CO)_5 \quad (6)$$

If the reaction were done in basic solution at the proper pH, the $Fe(CO)_4^{2-}$ would be protonated (3) and the $Fe(CO)_5$ would be converted to $HFe(CO)_4^-$ (4).

$$Fe(CO)_4^{2-} + H_2O \rightarrow HFe(CO)_4^- + OH^- \quad (7)$$

$$Fe(CO)_5 + OH^- \rightarrow HFe(CO)_4^- + CO_2 \quad (8)$$

The net result of the photoreaction would be conversion of $Fe_3(CO)_{11}^{2-}$ to three molecules of $HFe(CO)_4^-$.

$$Fe_3(CO)_{11}^{2-} + 3CO + OH^- + H_2O \rightarrow 3HFe(CO)_4^- + 2CO_2 \quad (9)$$

Our plan was to couple the photofragmentation of $Fe_3(CO)_{11}^{2-}$ (reaction 9) with Hieber's trimerization reactions (1 and 2). This would yield a cycle for a photochemical water-gas shift reaction (reaction 10) catalyzed by the iron carbonyl anions.

$$H_2O + CO \rightarrow H_2 + CO_2 \quad (10)$$

This paper reports the results of our study of the photochemistry of $Fe_3(CO)_{11}^{2-}$ and the application of this work to the water-gas shift reaction.

Experimental

The iron carbonyl anions decompose when exposed to air. All manipulations were carried out in a nitrogen atmosphere glove box or on a vacuum line. Solvents were rigorously dried by standard techniques (5).

$[Ni(NH_3)_6][Fe_3(CO)_{11}]$ was prepared by the method of Hieber and Brendal (4). This salt was used for the photolyses done in aqueous solution. The compound was dissolved in NaOH solution, and the Ni^{2+} was precipitated as $Ni(OH)_2$ and removed by filtration. This avoided the possibility of any interference by the Ni^{2+} during the photolysis. For photolyses in organic solvents the PPN^+ salt of $Fe_3(CO)_{11}^{2-}$ was used (PPN^+ = triphenylphosphineiminium cation). This salt was prepared by adding a solution of PPNCl in methanol to the solution of $Fe_3(CO)_{11}^{2-}$ prepared in the reaction of OH^- with $Fe_3(CO)_{12}$ (4). $PPN_2Fe_3(CO)_{11}$ was recrystallized in the following manner using a swivel-frit assembly on a vacuum line. The compound was dissolved in the minimum amount of hot CH_2Cl_2. Petroleum ether (30-60°) was vacuum distilled into the hot CH_2Cl_2 solution just to the point of $PPN_2Fe_3(CO)_{11}$ crystallization. Upon cooling, the

compound crystallized from the solution. The crystals were filtered and then washed with petroleum ether. If this procedure was done quickly, pure crystals of $PPN_2Fe_3(CO)_{11}$ could be obtained. However, $Fe_3(CO)_{11}^{2-}$ is oxidized slowly in CH_2Cl_2 to give $Fe_4(CO)_{13}^{2-}$. If $Fe_3(CO)_{11}^{2-}$ in CH_2Cl_2 solution was allowed to stand for long periods of time, then the tetranuclear dianion was found as an impurity in the recrystallized product.

Photolyses were done in special two-arm evacuable cells. $PPN_2Fe_3(CO)_{11}$ was placed in one side arm and organic solvents were vacuum distilled into the other side arm. Several freeze-pump-thaw cycles were used to degas the solvents. Only after this degassing was the solvent allowed to mix with the $PPN_2Fe_3(CO)_{11}$ in the other side arm. Thick-walled quartz or glass cells equipped with Kontes quick-release teflon valves were used for the photolyses done under CO pressure. Pressures up to 6 atmospheres were obtainable in these cells. All photolyses were done at room temperature.

Electronic absorption spectra and spectral changes were recorded with a Cary 17 spectrophotometer. Infrared spectra were recorded with a Perkin-Elmer 225 instrument. A 1000 watt high pressure Hg-Xe arc lamp in conjunction with Corning cutoff filters or interference filters and a low pressure Hg lamp were used for the irradiations.

Ferrioxalate actinometry was used for quantum yield determinations at 254, 313, and 366 nm (6). The procedure was modified to adopt the precautions recently suggested by Bowman and Demas (7).

Reineke actinometry was used for quantum yields at 504 nm (8). In all cases, the quantum yields were determined by monitoring the disappearance of the 485 nm band in $Fe_3(CO)_{11}^{2-}$.

When a 1 M NaOH solution containing $Fe_3(CO)_{11}^{2-}$ is irradiated ($\lambda < 313$ nm) the characteristic brown color of the dianion disappears to give a colorless solution. Accompanying this bleaching are a vigorous evolution of gases from the solution and the formation of a white precipitate. A mass spectral analysis of the gases formed in the photoreaction showed CO and H_2 were present. Quantitative measurements of the amount of CO or H_2 evolved were done as follows. The total volume of gas evolved in the reaction was measured by Toeppler pumping the stirred photolyzed solution into a known volume and manometrically measuring the pressure. The gases were then passed through a heated CuO column. This oxidized the H_2 to H_2O and the CO to CO_2. The H_2O was condensed in a Dry Ice-acetone cooled trap and the amount of CO_2 (which has considerable vapor pressure at -78°) was measured by Toeppler pumping into a known volume and measuring the pressure. The amount of H_2 was computed by differences from the total amount of gas and the amount of CO found. Typically, 0.03 - 0.08 moles of H_2 and CO_2 were collected and the measurements were reproducible to ± 10%. The extreme air sensitivity of the white precipitate led us to believe it was $Fe(OH)_2$ (9). To measure the amount of Fe(II) formed in strongly alkaline solution, the analytical reagent 4,7-dihydroxy-1,10-phenanthroline (G. Frederick

Smith Chemical Co.) was used. Schilt, Smith, and Heimbuch have described the use of this reagent (10). In a typical experiment, exhaustive photolysis of 2.5×10^{-7} moles of $Fe_3(CO)_{11}^{2-}$ analyzed for 4.75×10^{-7} moles of Fe(II). On the basis of this $Fe_3(CO)_{11}^{2-} \rightarrow$ 2Fe(II) stoichiometry one mole of an iron containing compound needs yet to be accounted for. That this remaining Fe is in the form of $Fe(CO)_4^{2-}$ can be shown. This is done by protonating (3) the $Fe(CO)_4^{2-}$ at pH 8 and then irradiating this hydride to see if $Fe_3(CO)_{11}^{2-}$ forms according to reaction (1) and (2). Upon adjusting the pH and irradiating, the colorless solution quickly turned brown. This brown product has an absorption band maximum at 485 nm which identifies it as $Fe_3(CO)_{11}^{2-}$ (1). Of course, when $Fe_3(CO)_{11}^{2-}$ was photolyzed in non-aqueous solvents the formation of $Fe(CO)_4^{2-}$ could be followed directly using infrared spectroscopy (ν_{CO} = 1750 cm^{-1}). Heiber has reported (1) that $Fe_3(CO)_{11}^{2-}$ slowly reacts with H_2O according to equation (11).

$$Fe_3(CO)_{11}^{2-} \xrightarrow{H_2O} 3Fe(OH)_2 + 4H_2 + 11CO \qquad (11)$$

Control experiments showed that corrections for this thermal reaction were unnecessary on the time scale of the photolysis experiments.

$Fe_3(CO)_{11}^{2-}$ in CH_3CN solution reacts in the dark at room temperature with PPh_3 when the phosphine is present in large excess. However, when the molar ratio of PPh_3 to $Fe_3(CO)_{11}^{2-}$ is kept below 5:1, the dark

reaction is negligible. When $Fe_3(CO)_{11}^{2-}$ is photolyzed (λ=504 nm) with a five-fold excess of PPh_3 in acetonitrile solution the disappearance of the $Fe_3(CO)_{11}^{2-}$ dianion is accompanied by the appearance of a yellow precipitate (11). This yellow precipitate is $Fe(CO)_3(PPh_3)_2$. An infrared spectrum of the compound in CH_3CN showed a single band at 1880 cm^{-1} in the carbonyl stretching region. For comparison, Clifford and Mukherjee reported that $Fe(CO)_3(PPh_3)_2$ has a CO band at 1884.4 cm^{-1} in CS_2 (12). The amount of $Fe(CO)_3(PPh_3)_2$ formed was determined gravimetrically. Because $Fe(CO)_3(PPh_3)_2$ is virtually insoluble in cold CH_3CN, the precipitate was merely filtered from a cold solution, dried, and then weighed. In a typical experiment, 0.05055 grams of $(PPN)_2Fe_3(CO)_{11}$ yielded 0.0377 grams of $Fe(CO)_3(PPh_3)_2$ upon exhaustive photolysis, i.e., one mole of the cluster produced 1.8 moles of $Fe(CO)_3(PPh_3)_2$. A mass spectral analysis of the gas above the photolysis solution showed that CO, but no H_2, was evolved in the reaction. A quantitative study using the Toeppler pump showed that essentially one mole of CO is formed for each mole of $Fe_3(CO)_{11}^{2-}$ starting material (2.4×10^{-2} mmole $PPN_2Fe_3(CO)_{11}$ gave 2.1×10^{-2} mmole CO).

Infrared spectroscopic monitoring of the photolysis of $Fe_3(CO)_{11}^{2-}$ with PPh_3 showed, in addition to the band at 1880 cm^{-1} due to $Fe(CO)_3(PPh_3)_2$, the appearance of a band at 1750 cm^{-1} due to $Fe(CO)_4^{2-}$ (13). In experiments where the CH_3CN had not been rigorously dried, bands at 2000, 1910, and 1880 cm^{-1} also appeared,

due to $HFe(CO)_4^-$ (13). No other carbonyl-stretching bands were present. In particular, the absence of bands at 2055, 1978, and 1943 cm^{-1} (12) and at 2064, 1976, and 1959 cm^{-1} (14) showed that neither $Fe(CO)_4PPh_3$ nor $Fe(CO)_4(CH_3CN)$ formed. Control experiments showed that $Fe(CO)_4(PPh_3)$ did not react with PPh_3 to give $Fe(CO)_3(PPh_3)_2$ when photolyzed at 504 nm. When the bidentate phosphine ligand dppe (1,2,-bis-(diphenylphosphino)-ethane) is used in this photoreaction rather than PPh_3, $Fe(CO)_3$ dppe forms. This product has bands at 1978, 1907, and 1888 cm^{-1} in the carbonyl region in CH_3CN solution. $Fe(CO)_3$ dppe has reported infrared frequencies at 1984, 1912, and 1890 cm^{-1} (15) in tetrachloroethylene solution.

When $PPN_2Fe_3(CO)_{11}$ is photolyzed ($\lambda > 320$ nm) in CH_2Cl_2 with no phosphine present, the products formed are $Fe(CO)_4^{2-}$ and $Fe_4(CO)_{13}^{2-}$ (1980 and 1950 cm^{-1}) (13). The addition of PPh_3 to the photolysis solution (100-fold molar excess) inhibited the formation of $Fe_4(CO)_{13}^{2-}$. In this case, as in CH_3CN, $Fe(CO)_4^{2-}$ and $Fe(CO)_2(PPh_3)_2$ were the carbonyl-containing products.

Discussion

Electronic Structure

The electronic absorption spectrum of $Fe_3(CO)_{11}^{2-}$ is shown in Figure 1. For comparison, the spectrum of $Fe_3(CO)_{12}$ is also displayed. Prominent in the $Fe_3(CO)_{11}^{2-}$ spectrum are a band at 485 nm and a shoulder at 340 nm. The spectrum may be interpreted

Figure 1

A comparison of the electronic absorption spectra of $Fe_3(CO)_{11}^{2-}$ and $Fe_3(CO)_{12}$. The spectra are for $Fe_3(CO)_{11}^{2-}$ in 1 M NaOH (——) and for $Fe_3(CO)_{12}$ in 2-methylpentane (----).

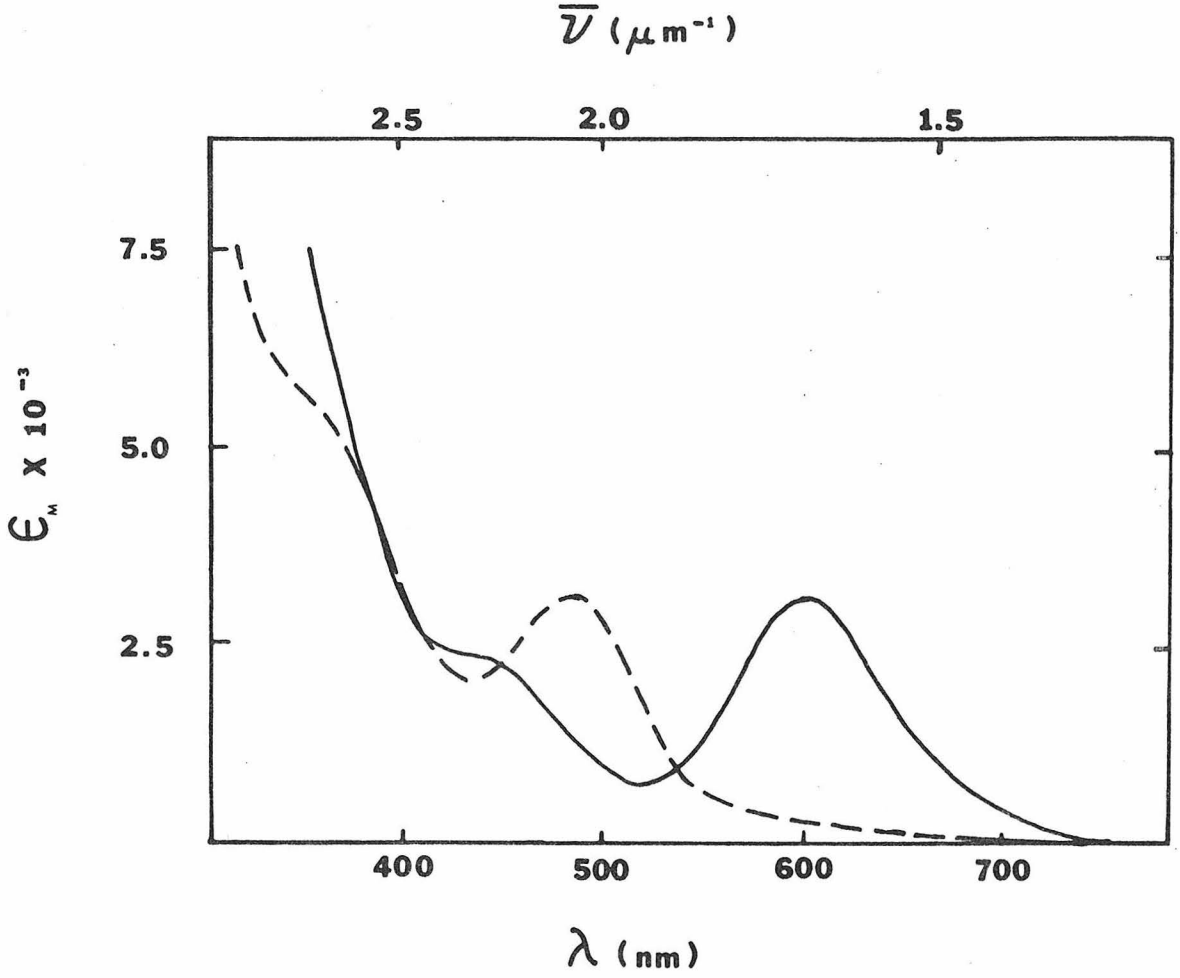
$\overline{\nu}$ (μm^{-1})
2.5
2.0
1.5
7.5
5.0
2.5
ϵ_M x 10^{-3}
400
500
600
700
λ (nm)

by reference to our work (16) on the electronic structure of the $M_3(CO)_{12}$ complexes (M = Fe, Ru, Os). Two electronic transitions in these trinuclear carbonyl complexes give rise to prominent absorption bands at relatively low energies. One transition is from a metal-metal bonding to antibonding orbital ($\sigma \rightarrow \sigma^*$) and the other is from a low-energy metal-metal antibonding level to σ^* ($\sigma^{*\prime} \rightarrow \sigma^*$). The $Fe_3(CO)_{11}^{2-}$ ion has a somewhat different structure than the $M_3(CO)_{12}$ molecules (17) (Figure 2), but the presence of two low-energy bands suggests that transitions related to $\sigma \rightarrow \sigma^*$ and $\sigma^{*\prime} \rightarrow \sigma^*$ still occur. The two bands in $Fe_3(CO)_{11}^{2-}$ have blue shifted with respect to their counterparts in $Fe_3(CO)_{12}$ (Figure 1). This finding rules out assignment of the two bands to low-energy MLCT transitions. As in $Fe_3(CO)_{12}$, we suggest assignment of the lowest energy band (485 nm) to the $\sigma^{*\prime} \rightarrow \sigma^*$ transition and the shoulder at 340 nm to $\sigma \rightarrow \sigma^*$.

Photochemistry

When $Fe_3(CO)_{11}^{2-}$ is irradiated in 1 M NaOH solution with uv light ($\lambda < 313$ nm), the products shown in reaction (12) are formed.

$$Fe_3(CO)_{11}^{2-} \xrightarrow[1\ M\ NaOH]{h\nu} Fe(CO)_4^{2-} + 2Fe(OH)_2 + 7CO + 2H_2 \qquad (12)$$

Figure 2

A comparison of the structure of $Fe_3(CO)_{12}$ (A) with $Fe_3(CO)_{11}^{2-}$ (B).

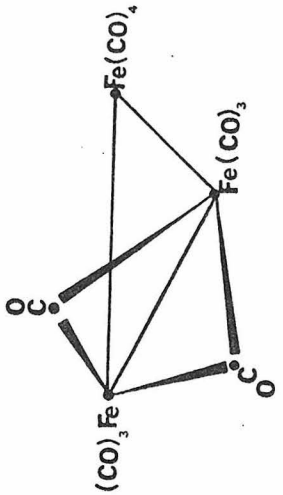

A

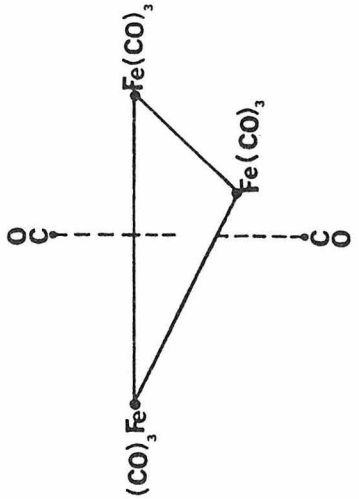

B

$H_2Fe(CO)_4$ is a diprotic acid with $pK_a(1) = 4.4$ and $pK_a(2) = 14$ (3). Therefore, the aqueous solution photolyses were done in strong base to avoid protonation of $Fe(CO)_4^{2-}$ and the subsequent photolysis of $HFe(CO)_4^-$ (reaction 1). Reaction 12 might proceed by the fragmentation outlined in reaction (4). The seven moles of CO come from the decomposition of the unstable carbonyl fragments, $Fe(CO)_4$ and $Fe(CO)_3$. The Fe(0) is oxidized to Fe(II) and the H_2 that forms is undoubtedly the reduction product (18). Attempts to trap the $Fe(CO)_3$ and the $Fe(CO)_4$ fragments with CO in aqueous solution failed. Even at 6 atm CO pressure, the solubility of CO in water is so low that the fragments cannot be trapped and conversion to Fe(II) is still observed. The quantum yields for reaction (12) at various wavelengths are given in Table 1. The mechanistic implications of these wavelength-dependent quantum yields are discussed later.

Carbon monoxide is considerably more soluble in CH_3CN than in water. Therefore, the photolysis of $Fe_3(CO)_{11}^{2-}$ under several atmospheres of CO was repeated using CH_3CN as the solvent. Under these conditions no photoreaction took place; CO inhibited the photofragmentation.

This meant that in order to trap the coordinately unsaturated fragments, it was necessary to use phosphines, rather than CO. Irradiation of an acetonitrile solution of $Fe_3(CO)_{11}^{2-}$ containing an excess of PPh_3 proceeds according to reaction (13).

Table 1. Wavelength Dependent Quantum Yields

$Fe_3(CO)_{11}^{2-}$ $\xrightarrow{1\ M\ NaOH}$	$Fe(CO)_4^{2-}$ +	$2Fe(OH)_2$ +	$7CO$ +	nH_2
Wavelength	504	366	313	254
Quantum yield	0	0	5.5×10^{-3}	1.1×10^{-2}

$Fe_3(CO)_{11}^{2-}$ $\xrightarrow{PPh_3}$	$Fe(CO)_4^{2-}$ +	$2Fe(CO)_3(PPh_3)_2$ +	CO
Wavelength	504	366	313	254
Quantum Yield	5.1×10^{-3}	5.0×10^{-3}	a	a

[a]Strong light absorption by the PPN^+ cation prohibited measurement at these wavelengths.

$$Fe_3(CO)_{11}^{2-} \xrightarrow[\lambda = 504\ nm]{PPh_3} 2Fe_3(CO)_3(PPh_3)_2 + CO + Fe(CO)_4^{2-} \qquad (13)$$

It is significant that no $Fe(CO)_4(PPh_3)$ is formed. Control experiments showed that $Fe(CO)_4(PPh_3)$ is not converted to $Fe(CO)_3(PPh_3)_2$ by irradiation at the wavelengths used in this experiment. This result and the observation that the reaction is inhibited by CO rule out the photolytic fragmentation pathway proposed in reaction (4). The quantum yields for reaction (13) are given in Table 1. These will be discussed later.

Equation 14 is our proposed pathway for the photofragmentation of $Fe_3(CO)_{11}^{2-}$. This pathway is consistent with the experimental observations, namely, that (a) CO inhibits the photochemical reaction; (b) no $Fe(CO)_4$ fragments are formed; (c) two moles of $Fe(CO)_3(PPh_3)_2$ are formed per mole of $Fe_3(CO)_{11}^{2-}$ and 1 mole of CO is evolved; and (d) the formation of $Fe(CO)_4^{2-}$ can be observed directly using infrared spectroscopy.

$$Fe_3(CO)_{11}^{2-} \underset{}{\overset{h\nu}{\rightleftharpoons}} CO + Fe_3(CO)_{10}^{2-}$$

$$Fe(CO)_4^{2-} + 2Fe(CO)_3 \leftarrow Fe_3(CO)_{10}^{2-}$$

$$2Fe(CO)_3 \xrightarrow{2PPh_3} 2Fe(CO)_3(PPh_3)_2 \qquad (14)$$

Thus, we propose that Fe-CO dissociation is the primary photoprocess, and only after the loss of a CO molecule will the trinuclear cluster undergo fragmentation. The aqueous solution photochemistry discussed earlier is also consistent with the pathway given in equation (14). The two moles of Fe(II) come from the decomposition of the two unstable $Fe(CO)_3$ fragments and seven moles of CO are still evolved in (14) if no trapping agent is present. Indeed, this is the case when $Fe_3(CO)_{11}^{2-}$ is photolyzed in CH_3CN in the absence of PPh_3. The only iron-carbonyl product is $Fe(CO)_4^{2-}$. Acetonitrile is a good trapping agent for $Fe(CO)_4$ fragments (14); thus the observation that no $Fe(CO)_4(CH_3CN)$ is formed in the photolysis is also consistent with reaction (14).

Photolysis of $Fe_3(CO)_{11}^{2-}$ in CH_2Cl_2 gave $Fe_4(CO)_{13}^{2-}$ in addition to $Fe(CO)_4^{2-}$. The tetranuclear cluster is probably formed by attack of an $Fe(CO)_3$ fragment on a $Fe_3(CO)_{11}^{2-}$ molecule. This results in substitution of a CO group by $Fe(CO)_3$.

$$Fe_3(CO)_{11}^{2-} + Fe(CO)_3 \rightarrow Fe_4(CO)_{13}^{2-} + CO \qquad (15)$$

Such a reaction is likely in view of the fact (19) that $Fe(CO)_5$ reacts with $Fe_3(CO)_{11}^{2-}$ at elevated temperatures to produce $Fe_4(CO)_{13}^{2-}$.

$$Fe_3(CO)_{11}^{2-} + Fe(CO)_5 \rightarrow Fe_4(CO)_{13}^{2-} + 3CO \qquad (16)$$

Dissociation of CO from $Fe(CO)_5$ is known to occur readily at high temperatures, so the thermal reaction probably also proceeds by attack of an $Fe(CO)_x$ fragment on $Fe_3(CO)_{11}^{2-}$. The point here is that no new photochemical mechanism is necessary to account for the formation of $Fe_4(CO)_{13}^{2-}$ when CH_2Cl_2 is the solvent. Further evidence that CO dissociation is still the primary photoprocess in CH_2Cl_2 is our observation that one atmosphere of CO inhibits the photoreaction in CH_2Cl_2.

Why do we see $Fe_4(CO)_{13}^{2-}$ in CH_2Cl_2, but not in H_2O, CH_3CN, or acetone? The following result provides a clue to this behavior: photolysis of $Fe_3(CO)_{11}^{2-}$ in CH_2Cl_2 with excess PPh_3 does not give $Fe_4(CO)_{13}^{2-}$. Rather, $Fe(CO)_3(PPh_3)_2$ and the other products in reaction (13) are formed. Obviously, if the $Fe(CO)_3$ fragment is trapped, as it can be with PPh_3, it cannot react with a $Fe_3(CO)_{11}^{2-}$ molecule. This suggests that the $Fe(CO)_3$ fragment is weakly trapped in CH_3CN, acetone, and H_2O. These three solvents all have the ability to coordinate and might form unstable complexes of the type $Fe(CO)_3(solvent)_2$. On the other hand, CH_2Cl_2 is not a coordinating solvent and so the $Fe(CO)_3$ fragment is, in effect, trapped by a $Fe_3(CO)_{11}^{2-}$ molecule to give $Fe_4(CO)_{13}^{2-}$.

It remains to discuss why Fe-CO dissociation is the favored pathway rather than a metal-metal bond cleavage photofragmentation process. As mentioned previously, the lowest energy electronic excited states of trinuclear carbonyl complexes involve population

of a metal-metal antibonding orbital. Numerous studies of dinuclear carbonyl complexes have shown (20) that excitations that result in occupation of the metal-metal σ^* orbital lead to homolytic cleavage of the metal-metal bond. While it has never been shown, it is suspected that the primary photoprocess in trinuclear carbonyl complexes is homolytic cleavage of one metal-metal bond to yield a diradical excited state complex (20).

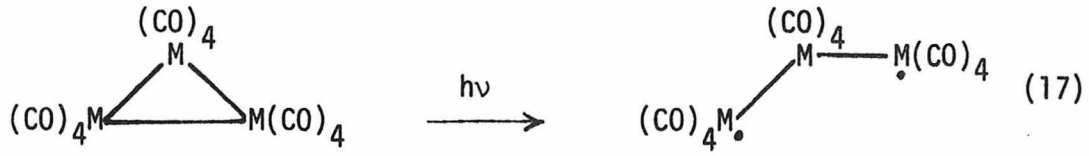

(17)

In trinuclear clusters without bridging groups, such as $Ru_3(CO)_{12}$, electronic excitation is sufficient to initiate complete fragmentation of the molecule (2). Fragmentation probably occurs because a large structural change occurs after the excitation. This change in structure does not allow for facile reformation of the M-M bond. However, in molecules with bridges, such as $Fe_3(CO)_{11}^{2-}$ (17), the structure is more rigid and large changes in geometry cannot occur. Thus, reformation of the metal-metal bond is favored. Of course, CO dissociation from the diradical excited state leads to the reaction pathway proposed in equation (14). The extremely low quantum yields for reaction (13) (Table II) suggest that Fe-CO dissociation is not an efficient process compared to recombination of the diradical electrons to form the metal-metal bond.

Table 1 shows that the two lowest energy transitions in $Fe_3(CO)_{11}^{2-}$ are photochemically inactive in 1 M NaOH solution. Irradiation with wavelengths shorter than 313 nm is required for reaction (12) to occur. The electronic transitions at these higher energies almost certainly have some M-CO antibonding character. Thus, rather than going through the diradical intermediate proposed in (17), it seems likely that Fe-CO dissociation occurs as a direct result of the electronic excitation. However, the two lowest energy transitions are photochemically active in acetonitrile solution (reaction 13). In this reaction, the intermediate formed by dissociation of CO from the "diradical" excited complex would be stabilized by coordination of either a solvent molecule or a PPh_3 molecule at the empty coordination site.

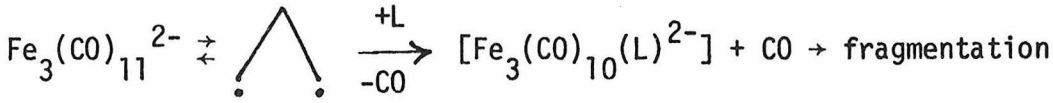

(L = PPh_3 or CH_3CN)

Stabilization of the CO-dissociated intermediate in this way would not be as likely in aqueous solution so rapid recombination of the diradical occurs and no photochemistry is observed.

Several other examples of metal-CO dissociation rather than fragmentation in complexes which have ligands bridging the metal-

metal bonds are found in the literature. Von Gustorf has shown that $Fe_3(CO)_{10}NSi(CH_3)_3$ photochemically substitutes H_2 or PR_3 for CO without any fragmentation (21). Recent work in our laboratory has shown that homolytic cleavage of the FeFe bridged unit does not occur when $Cp_2Fe_2(CO)_4$ is irradiated (22) and other workers have shown that $HCCo_3(CO)_9$ photochemically substitutes PPh_3 for CO (23). From these examples and our own results it is apparent that metal-CO dissociation is an important pathway in molecules with bridging ligands. Carbonyl dissociation may also be a more important pathway than is now recognized even for cluster complexes without bridging ligands. For instance, Johnson, et al., have proposed (2) that in addition to metal-metal bond cleavage, Ru-CO dissociation followed by fragmentation is a primary process in the photoreaction of $Ru_3(CO)_{12}$ with phosphines.

Unfortunately, Fe-CO dissociation, rather than fragmentation also means that $Fe_3(CO)_{11}^{2-}$ cannot be used as a photocatalyst in the water-gas shift reaction. However, we have noted that CO reacts with $Fe_3(CO)_{11}^{2-}$ in acetonitrile solution in a dark reaction according to reaction (15).

$$Fe_3(CO)_{11}^{2-} \xrightarrow[CH_3CN]{CO,\ 6\ atm} Fe_2(CO)_8^{2-} + Fe(CO)_5 \qquad (15)$$

This reaction, followed by reaction (8), would fit into the cycle proposed in the introduction to this paper. Reaction (15) does

not take place in aqueous solution under 6 atm pressure presumably because of the lower solubility of CO in water. In order to completely couple reaction (15) with reactions (1) and (2), perhaps a CH_3CN-H_2O mixed solvent could be used at slightly higher CO pressure.

Finally, we wish to point out that besides being potentially useful in catalyzing the water-gas shift reaction, the photochemical fragmentation of $Fe_3(CO)_{11}^{2-}$ does produce $Fe(CO)_3$ fragments. The behavior of multiple coordinately unsaturated fragments is of current interest in chemistry but such fragments are not always easily produced. Photolysis of polynuclear clusters and particularly of ionic clusters might be an easy route to these fragments. Besides being interesting from a mechanistic viewpoint, multiple coordinately unsaturated fragments have some synthetic utility. For instance, use of the bidentate phosphine dppe in reaction 13 rather than PPh_3 yields $Fe(CO)_3$(dppe), a molecule not easily synthesized by conventional routes (15).

References and Notes

1. W. Hieber and E. F. Schubert, Z. Anorg. Allg. Chem., 338, 32 (1965).
2. B. F. G. Johnson, J. Lewis, and M. V. Twigg, J. Organomet. Chem., 67, C75 (1974).
3. W. Hieber and W. Hübel, Z. Elekt., 57, 235 (1953).
4. W. Hieber and G. Brendal, Z. Anorg. Allg. Chem., 289, 324 (1957).
5. D. D. Perrin, W. L. F. Armarego, and D. R. Perrin, Purification of Laboratory Chemicals, Pergamon Press, London, 1966.
6. J. G. Calvert and J. N. Pitts, Photochemistry, John Wiley and Sons, Inc., New York, 1966.
7. W. D. Bowman and J. N. Demas, J. Phys. Chem., 80, 2434 (1976).
8. E. E. Wegner and A. W. Adamson, J. Am. Chem. Soc., 88, 394 (1966).
9. F. A. Cotton and G. Wilkinson, Advanced Inorganic Chemistry, 3rd ed., Interscience, New York (1972), p. 860.
10. A. A. Schilt, G. F. Smith, and A. Heimbuch, Anal. Chem., 28, 806 (1956).
11. The disappearance of the $Fe_3(CO)_{11}^{2-}$ was monitored by following the disappearance of the electronic absorption band at 504 nm. This band has shifted in CH_3CN from its value of 485 nm in 1 M NaOH. We suggest that this shift might be due to ion-pairing of the counter-ion with the $Fe_3(CO)_{11}^{2-}$ complex.

12. A. F. Clifford and A. K. Mukherjee, Inorg. Chem., 2, 151 (1963).

13. W. F. Edgell, M. T. Yang, B. J. Bulkin, R. Bayer, and N. Koizumi, J. Am. Chem. Soc., 87, 3080 (1965).

14. E. H. Schubert and R. K. Sheline, Inorg. Chem., 5, 1071 (1966).

15. F. Zingales, F. Canziani, and R. Ugo, Chim. Ind. (Milan), 44, 1394 (1962).

16. D. R. Tyler, R. A. Levenson, and H. B. Gray, J. Am. Chem. Soc., in press.

17. (a) O. S. Mills, A. A. Hock, and G. Robinson, Abstract A, XVIIth Internat. Cong. Pure Appl. Chem., Munich, 143 (1959); (b) K. Farmery, M. Kilner, R. Greatrex, and N. N. Greenwood, J. Chem. Soc. (A), 2339 (1969).

18. The amount of H_2 formed was never stoichiometric for some unexplained reason. In our early experiments when the acetonitrile was not rigorously dried, the $Fe(CO)_4^{2-}$ was protonated to give $HFe(CO)_4^-$ which was probably photolyzed during the Toeppler pumping to give excess ($n > 2$) H_2 (reaction 1). In later experiments with dry CH_3CN, n was found to be $\simeq$ 1.5.

19. W. Hieber and E. H. Schubert, Z. Anorg. Allg. Chem., 338, 37 (1965).

20. M. S. Wrighton, Topics in Current Chem., 65, 68 (1977).

21. I. Fischler, R. Wagner, E. A. Koerner von Gustorf, J. Organometl. Chem., 112, 155 (1976).

22. D. R. Tyler and H. B. Gray, unpublished work.

23. G. L. Geoffroy and R. A. Epstein, Inorg. Chem., 16, 2795 (1977).

CHAPTER 4

The Photochemistry of $(h^5\text{-}C_5H_5)_2Fe_2(CO)_4$

Abstract: $Cp_2Fe_2(CO)_4$ (Cp = h^5-C_5H_5) reacts photochemically with PR_3 (R = Ph, OiPr) to give only monosubstituted product, $Cp_2Fe_2(CO)_3(PR_3)$. A reaction intermediate can be trapped by photolyzing $Cp_2Fe_2(CO)_4$ in the presence of $P(OiPr)_3$ at -78° C in ethyl chloride or THF solution. The infrared spectrum of the intermediate has $\nu(C\equiv O)$ = 1720 cm^{-1}, and its electronic spectrum does not exhibit a $\sigma \rightarrow \sigma^*$ band. The evidence suggests that the intermediate is $Cp(CO)_2Fe\text{-}CO\text{-}Fe(CO)(P(OiPr)_3)Cp$, a molecule in which a single CO bridges the Fe atoms and in which there is no direct Fe-Fe bond. The mechanism of the photoreaction of PR_3 with $Cp_2Fe_2(CO)_4$ is proposed to involve formation of the CO-bridged intermediate, $Cp_2Fe_2(CO)_4(PR_3)$, followed by loss of CO to give the product, $Cp_2Fe_2(CO)_3(PR_3)$. Evidence is also presented that the coordinately-unsaturated intermediate, $Cp(CO)_2Fe\text{-}CO\text{-}Fe(CO)Cp$, is involved in the reactions of $Cp_2Fe_2(CO)_4$ with $Mn_2(CO)_{10}$ and CCl_4 to give $(CO)_5Mn\text{-}Fe(CO)_2Cp$ and $CpFe(CO)_2Cl$, respectively.

Photolysis of $Ru_3(CO)_{12}$ in the presence of π-acceptor ligands results in monomeric products of the type $Ru(CO)_4L$ (L = PR_3, CO, C_2H_4) (1). We have recently shown that the lowest energy electronic excited states of $Ru_3(CO)_{12}$ involve electronic population of a molecular orbital which is metal-metal antibonding (2). Thus, it has been proposed that the initial step in the photofragmentation of $Ru_3(CO)_{12}$ is homolytic cleavage of one Ru-Ru bond (3). Presumably, the "diradical" thus produced fragments further to give three $Ru(CO)_4$ fragments which react with the ligand L to give the product. In contrast to this fragmentation mechanism is the photochemical fragmentation of $Fe_3(CO)_{11}^{2-}$, a triangular complex with two face-bridging CO groups (4). In our study of the photochemistry of this cluster, we found that the initial reaction step is dissociation of CO from the cluster (5). Subsequent to this dissociation, the unstable $Fe_3(CO)_{10}^{2-}$ fragments and three monomeric fragments are formed. To explain the different photochemical behavior of the bridged and unbridged trinuclear clusters, we proposed that the Fe-C-Fe bonds of the face-bridging carbonyl ligands prevented fragmentation of the $Fe_3(CO)_{11}^{2-}$ excited state.

It is clear that bridging ligands can influence the photochemical behavior of metal cluster complexes. Therefore, we decided to investigate more fully the effects of bridging carbonyl ligands

on the photochemical reaction pathways of metal-metal bonded complexes. Herein we report the results of our study on the photochemistry of $Cp_2Fe_2(CO)_4$ (Cp = h^5-C_5H_5), a molecule in which the Fe-Fe unit is bridged by two carbonyls (6). Of particular interest to us was whether excitation of this molecule would produce two identical 17-electron fragments, eq. (1), as is the case for unbridged metal-metal bonded dimers (3),

$$Cp_2Fe_2(CO)_4 \xrightarrow{h\nu} 2CpFe(CO)_2 \qquad (1)$$

or whether the bridging CO ligands would prevent fragmentation of the dimer and some other reaction pathway would occur. A preliminary account of this work has appeared (7).

Experimental

$Cp_2Fe_2(CO)_4$ was purchased from ROC/RIC Chemical Corp. Phosphine and phosphite derivatives of the type $Cp_2Fe_2(CO)_3PR_3$ were prepared by the method of Haines and Du Preez (8). Triphenylphosphine (PPh_3) and trimethylphosphite ($P(OMe)_3$) were purchased from MCB Chemical Co. Tri-n-butylphosphine ($P(n\text{-}C_4H_9)_3$) and triisopropyl phosphite ($P(OiPr)_3$) were purchased from Aldrich Chemical Co. Ethyl chloride (Eastman) and other spectroquality solvents were used as received without further purification.

Electronic absorption spectra and spectral changes were recorded with a Cary 17 spectrophotometer. Infrared spectra were recorded with a Perkin-Elmer 225 instrument. A 1000 Watt high pressure Hg-Xe arc lamp,in conjunction with Corning cut-off filters, was used for the irradiations. EPR spectra were recorded with a Varian E-line Century Series spectrometer, equipped with a 12 inch magnet. Temperature regulation was provided by an Air Products Heli-Trans system and frequencies were determined with a PRD Electronics, Inc. frequency meter.

Ferrioxalate actinometry was used for quantum yield determinations at 254, 313, and 366 nm (9). The procedure was modified to adopt the precautions recently suggested by Bowman and Demas (10). Reineke actinometry was used for quantum yields at 450 and 504 nm (11). In all cases, the quantum yields were determined by monitoring the disappearance of the 520 nm band in $Cp_2Fe_2(CO)_4$. The absorption spectra of the phosphine substitution products, $Cp_2Fe_2(CO)_3PR_3$, overlap with the spectrum of $Cp_2Fe_2(CO)_4$ at 520 nm. Thus, to minimize the error in the quantum yield measurement of the substitution reaction, only the first 10% of the reaction was monitored. At such small conversions the absorption by the product is small.

Low temperature photolyses were done in a beaker filled with a Dry Ice-acetone mixture.

$Cp_2Fe_2(CO)_2(P(OMe)_3)_2$ was synthesized by photolyzing a benzene solution of $Cp_2Fe_2(CO)_4$ containing excess $P(OMe)_3$. After several

hours of irradiation, the solution was concentrated and cooled. The greenish-black $Cp_2Fe_2(CO)_4$ crystals were filtered from solution and dried in vacuo. Anal. Calcd. for $C_{18}H_{28}Fe_2O_8P_2$: C, 39.6; H, 5.13; P, 11.34. Found: C, 39.45; H, 5.14; P, 11.22. $Cp_2Fe_2(CO)_2(P(OMe)_3)_2$ has carbonyl infrared bands at 1718 and 2012 cm^{-1} in cyclohexane.

Photolyses were done in special two-arm evacuable cells equipped with Kontes quick-release valves. One side was a glass bulb and the other side was a quartz spectrophotometer cell. Photolysis solutions in the glass bulb were degassed by three freeze-pump-thaw cycles. By tipping the apparatus, the solution ran over into the quartz cell and the electronic spectrum could be monitored. Thick-walled quartz or glass cells equipped with Kontes quick-release valves were used for the photolyses done under CO pressure. Pressures up to 6 atmospheres were obtainable in these cells.

Results

Substitution Photochemistry

Figure 1 shows the electronic spectral changes accompanying the photolysis of $Cp_2Fe_2(CO)_4$ with triisopropyl phosphite in cyclohexane to give $Cp_2Fe_2(CO)_3P(OiPr)_3$. The infrared spectrum of the product has carbonyl stretching bands at 1757, 1939, and 1961 cm^{-1} in cyclohexane solution. These band positions are in close agreement with the literature values for $Cp_2Fe_2(CO)_3P(OiPr)_3$

Figure 1

Spectral changes upon irradiation ($\lambda \geq 500$ nm) of 1.5×10^{-3} M $Cp_2Fe_2(CO)_4$ in the presence of 0.3 M $P(OiPr)_3$ in cyclohexane solution at room temperature. The disappearance quantum yield for 504 nm excitation is 0.045. A similar photoreaction is observed with PPh_3 as the entering group. In each case the same reaction is observed for 366 nm excitation. Observed conversions to $Cp_2Fe_2(CO)_3(PR_3)$ are 98 ± 2% (R = Ph) and 87 ± 5% (R = OiPr).

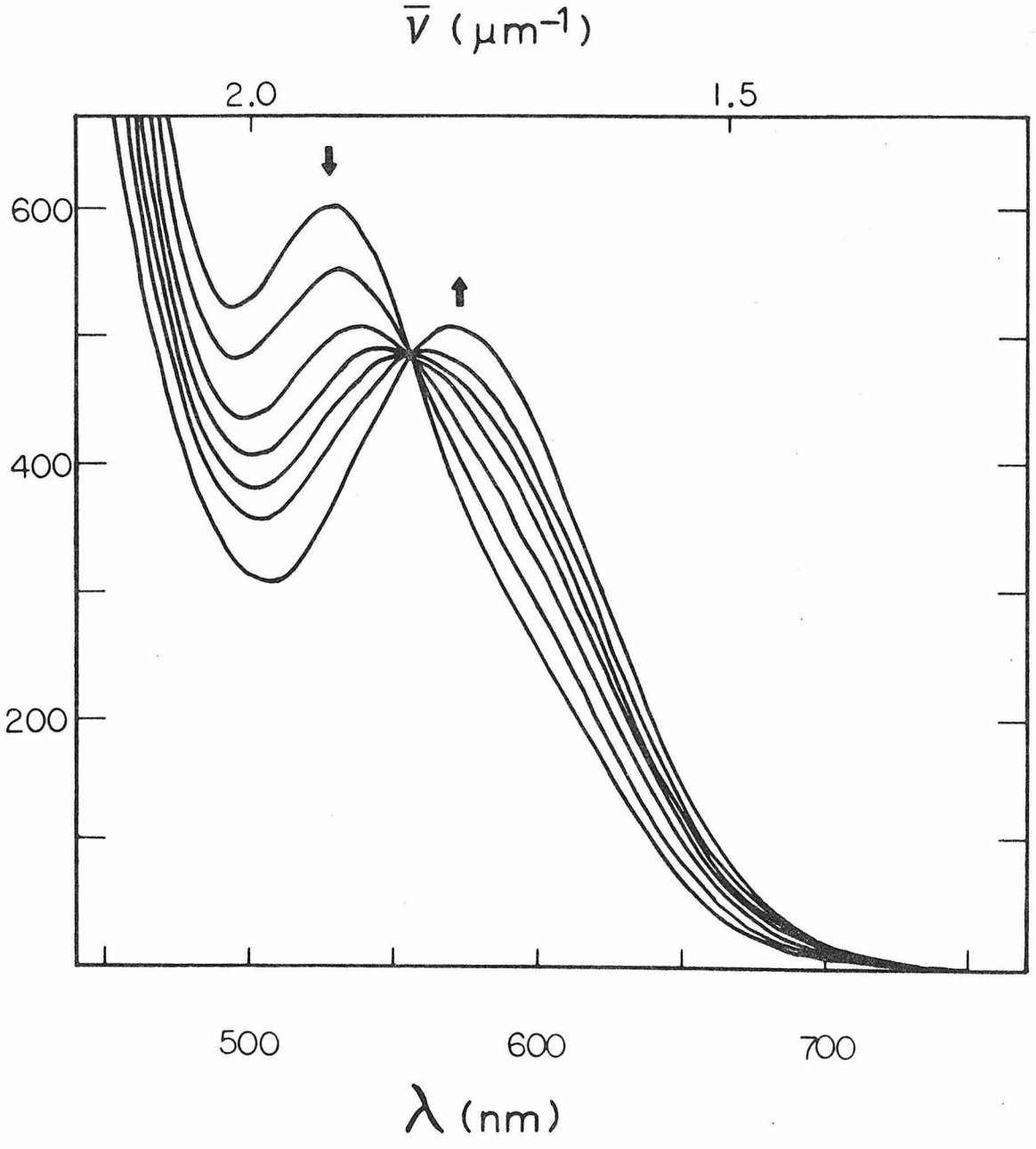
$\bar{\nu}$ (μm^{-1})
2.0
1.5
600
400
200
500
600
700
λ (nm)

reported by Haines and Du Preez (8). Using our measured values of 590 M^{-1} cm^{-1} and 610 M^{-1} cm^{-1} for the extinction coefficients of the lowest energy electronic bands in $Cp_2Fe_2(CO)_3P(OiPr)_3$ and $Cp_2Fe_2(CO)_4$, respectively, we calculate 87% conversion of $Cp_2Fe_2(CO)_4$ to $Cp_2Fe_2(CO)_3P(OiPr)_3$. It is not surprising that slightly less than quantitative conversion occurs because the absorption spectra of $Cp_2Fe_2(CO)_4$ and the monosubstituted product overlap. Irradiation of a solution of $Cp_2Fe_2(CO)_3(P(OiPr)_3)$ at the wavelengths used to photolyze $Cp_2Fe_2(CO)_4$ confirmed that the monosubstituted dimer slowly decomposes when irradiated. The decomposition products were not identified. Spectral changes similar to those in Figure 1 occur for PPh_3 and tri-n-butylphosphine. Once again, a comparison of the infrared spectra of the products to the literature spectra confirms that the monosubstituted dimers are the only products (8). No disubstituted products were obtained with these phosphines.

Photolysis of $Cp_2Fe_2(CO)_4$ with $P(OMe)_3$ leads to quantitative conversion to $Cp_2Fe_2(CO)_4(P(OMe)_3)_2$:

$$Cp_2Fe_2(CO)_4 + 2P(OMe)_3 \xrightarrow[\lambda \geq 366]{h\nu} Cp_2Fe_2(CO)_2(P(OMe)_3)_2 + 2CO$$

The formation of the monosubstituted dimer as an intermediate in this reaction was not observed spectroscopically.

The quantum yield for the reaction of phosphines or phosphites with $Cp_2Fe_2(CO)_4$ is dependent upon the phosphine concentration. A Stern-Volmer plot is shown in Figure 2. In an attempt to trap an intermediate in this reaction, we photolyzed ($\lambda \geq 366$ nm) a solution of $Cp_2Fe_2(CO)_4$ and triisopropyl phosphite in ethyl chloride at -78° (13). At this low temperature the green color characteristic of $Cp_2Fe_2(CO)_3P(OiPr)_3$ does not appear but rather an intermediate forms which is yellow in color. A yellow intermediate also forms with $P(C_4H_9)_3$ and $P(OMe)_3$. Upon warming the solution to room temperature, the yellow intermediate disappears and the solution turns green. An infrared spectrum shows that the green product is either the monosubstituted dimer (PR_3 = $P(OiPr)_3$ and $P(C_4H_9)_3$) or the disubstituted dimer (PR_3 = $P(OMe)_3$).

The electronic spectrum monitored during the low temperature photolysis of $Cp_2Fe_2(CO)_4$ with $P(OiPr)_3$ shows the disappearance of the bands due to $Cp_2Fe_2(CO)_4$. Eventually, the spectrum consists only of a rising absorption into the ultraviolet region of the spectrum. This is the spectrum of the yellow intermediate. No bands or shoulders are discernible between 300 and 800 nm. Upon warming the solution, the electronic spectrum of $Cp_2Fe_2(CO)_3P(OiPr)_3$ grows in. The infrared spectrum of the yellow intermediate in THF at -78° shows a band at 1720 cm^{-1}. The EPR spectrum of the intermediate, checked to temperatures as low as 15 K, had no signals. Finally, we note that if phosphine is not present in the low

Figure 2

A Stern-Volmer plot (Φ^{-1} vs. $[PPh_3]^{-1}$) for the photoreaction of $Cp_2Fe_2(CO)_4$ with PPh_3 in toluene solution at room temperature (λ = 366 nm). At very high $[PPh_3]$, a limiting value of Φ is reached. In benzene solution, Φ = 0.05 for 0.1 M PPh_3 (7). Values of Φ are referenced to 0.05 as the upper limit.

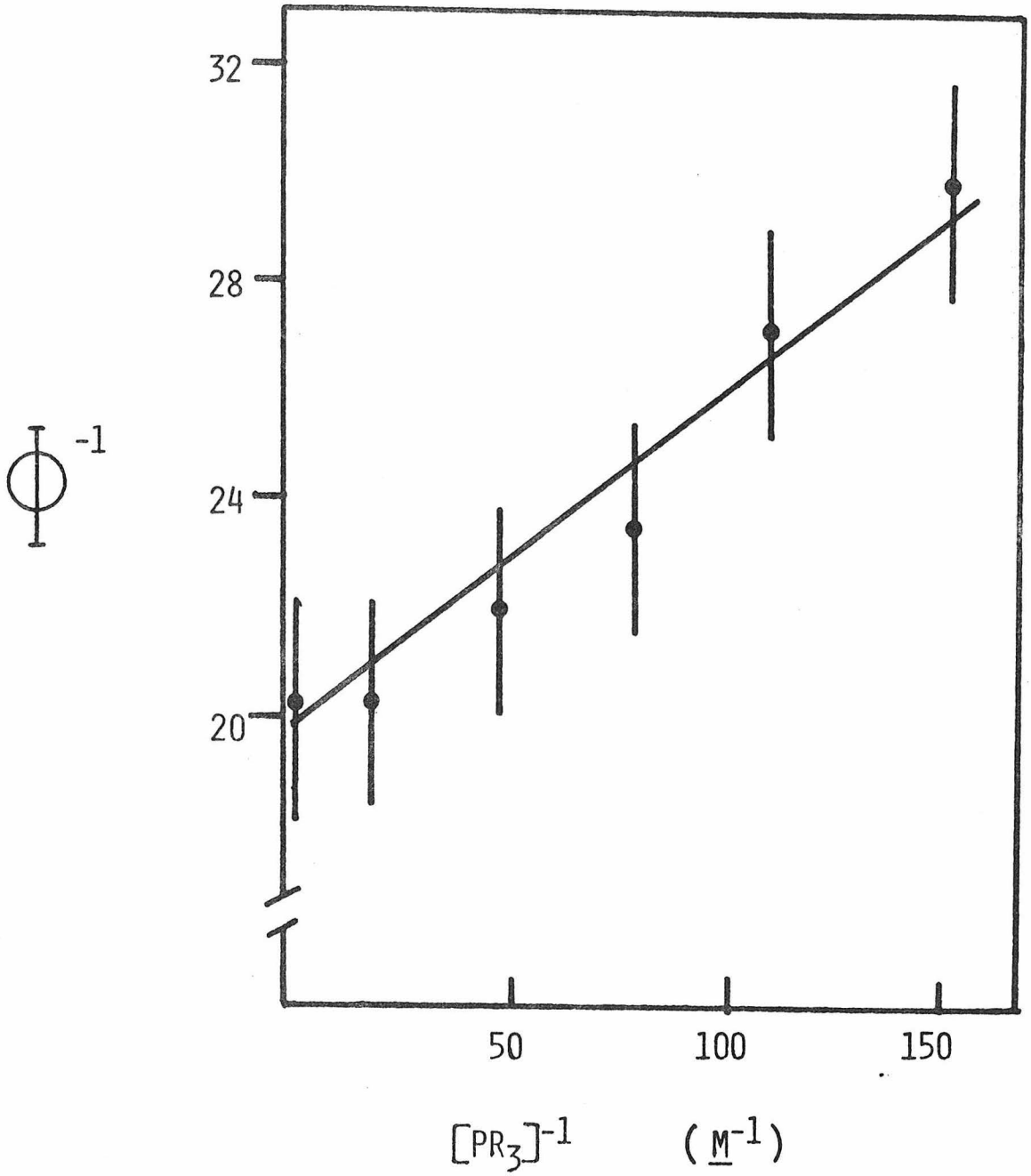
32
28
24
20
-1
50
100
150
$[PR_3]^{-1}$ ($\underline{M}^{-1}$)

temperature photolysis solution then the yellow intermediate does not form.

Non-Substitution Photochemistry

Homolytic cleavage at the bridged Fe-Fe unit in $Cp_2Fe_2(CO)_4$ would yield two $CpFe(CO)_2$ 17-electron fragments. Such fragments are usually identified as reaction intermediates by their chemical reactivity. For example, 17-electron fragments can abstract chlorine atoms from chlorocarbon solvents to give metal chloride complexes (3). As a test to determine if $CpFe(CO)_2$ is an intermediate in the photolysis of $Cp_2Fe_2(CO)_4$, we irradiated solutions of $Cp_2Fe_2(CO)_4$ in CCl_4 or $CHCl_3$. The chlorine abstraction product does indeed form.

$$Cp_2Fe_2(CO)_4 \xrightarrow[\lambda \geq 313 \text{ nm}]{CCl_4 \text{ or } CHCl_3} 2CpFe(CO)_2Cl \qquad (2)$$

$CpFe(CO)_2Cl$ was identified by its infrared spectrum in the carbonyl region (2012 and 2060 cm^{-1} in $CHCl_3$) (14). The quantum yields for reaction (2) in CCl_4 and $CHCl_3$ at various wavelengths are reported in the Table. The quantum yields are corrected for the dark reaction of $Cp_2Fe_2(CO)_4$ with the solvent (14). We found that reaction (2) is inhibited by excess CO. For example, under six atmospheres of CO pressure, there was no reaction between $Cp_2Fe_2(CO)_4$ and $CHCl_3$ after ten minutes of irradiation ($\lambda \geq 313$). Under the

Table. Quantum Yield Data

Wavelength	Reactants ($Cp_2Fe_2(CO)_4$ +)	Product	Φ[a]
366 nm	CCl_4	$CpFe(CO)_2Cl$	0.42
	$CHCl_3$	$CpFe(CO)_2Cl$	0.19
	PR_3[b]	$Cp_2Fe_2(CO)_3PR_3$	0.11
450 nm	CCl_4	$CpFe(CO)_2Cl$	0.11
	$CHCl_3$	$CpFe(CO)_2Cl$	0.075
	PR_3	$Cp_2Fe_2(CO)_3PR_3$	0.065
505 nm	CCl_4	$CpFe(CO)_2Cl$	0.067
	$CHCl_3$	$CpFe(CO)_2Cl$	0.074
	PR_3	$Cp_2Fe_2(CO)_3PR_3$	0.045

[a] Quantum yield of disappearance of $Cp_2Fe_2(CO)_4$.

[b] $PR_3 = P(O\text{-}iC_3H_7)_3$ in 1000 fold excess.

same conditions but with no added CO, complete conversion to $CpFe(CO)_2Cl$ would have occurred.

Cross-coupling reactions have also been used to identify 17-electron fragments as possible reaction intermediates. Photolysis of a cyclohexane solution of $Cp_2Fe_2(CO)_4$ and $Mn_2(CO)_{10}$ gives a yellow product with infrared carbonyl stretches at 2082, 2053, 2015, 1993, 1975 and 1945 cm^{-1}. This yellow product was identified as the cross-coupled dimer, $(CO)_5Mn\text{-}Fe(CO)_2Cp$, by comparison of its infrared spectrum to the reported literature spectrum (15). As other authors have noted (3), a 17-electron fragment cross-coupling mechanism requires that the product dimer form only when both reactant dimers are irradiated simultaneously. This is the case above. Irradiation of the solution at wavelengths where only $Cp_2Fe_2(CO)_4$ absorbs but not $Mn_2(CO)_{10}$ ($\lambda \geq 500$ nm) produces no net photolysis.

The other cross-coupling reactions which we investigated are shown in reactions (3) and (4).

$$Cp_2Fe_2(CO)_4 + Cp_2Fe_2(CO)_2(P(OMe)_3)_2 \xrightarrow[\lambda \geq 366 \text{ nm}]{h\nu} Cp_2Fe_2(CO)_3P(OMe)_3 \quad (3)$$

$$2Cp_2Fe_2(CO)_3P(OMe)_3 \xrightarrow[\lambda \geq 366 \text{ nm}]{h\nu} Cp_2Fe_2(CO)_2(P(OMe)_3)_2 + Cp_2Fe_2(CO)_4 \quad (4)$$

In each case, the disappearance of the starting materials and the appearance of the products were followed by infrared spectroscopy (8).

When a CH_2Cl_2 solution of $Cp_2Fe_2(CO)_4$ ($\approx 10^{-3}$ M) containing equimolar concentrations ($\approx$0.1 M) of CCl_4 and PPh_3 (or $P(OMe)_3$) is irradiated, the only product is $CpFe(CO)_2Cl$. A similar result holds when equimolar concentrations of $CHCl_3$ and phosphine are irradiated.

Discussion

We propose that $Cp_2Fe_2(CO)_4$ reacts photochemically by the reaction pathway in Figure 3. To rationalize this pathway it is first necessary to examine the electronic excited states of $Cp_2Fe_2(CO)_4$. The electronic spectrum of $Cp_2Fe_2(CO)_4$ has been reported (16). The spectrum has an intense near-uv band at 345 nm attributable to the $\sigma \rightarrow \sigma^*$ transition. The bands to lower energy are probably $d\pi \rightarrow \sigma^*$ transitions (3). With unbridged dimers it has been shown that electronic excitation into the σ^* orbital weakens the metal-metal bond and this is why homolytic cleavage of that bond occurs (3). Similarly, we might expect that irradiation into the $d\pi \rightarrow \sigma^*$ and $\sigma \rightarrow \sigma^*$ bands of $Cp_2Fe_2(CO)_4$ will weaken the Fe-Fe bond thereby giving the excited state which we have denoted by I*.

That excitation of $Cp_2Fe_2(CO)_4$ does not initially cleave the entire Fe-Fe bridged unit is shown by the phosphine substitution results. Consider the following. Kidd and Brown have recently

Figure 3

The proposed reaction pathway for the photoreactions of $Cp_2Fe_2(CO)_4$.

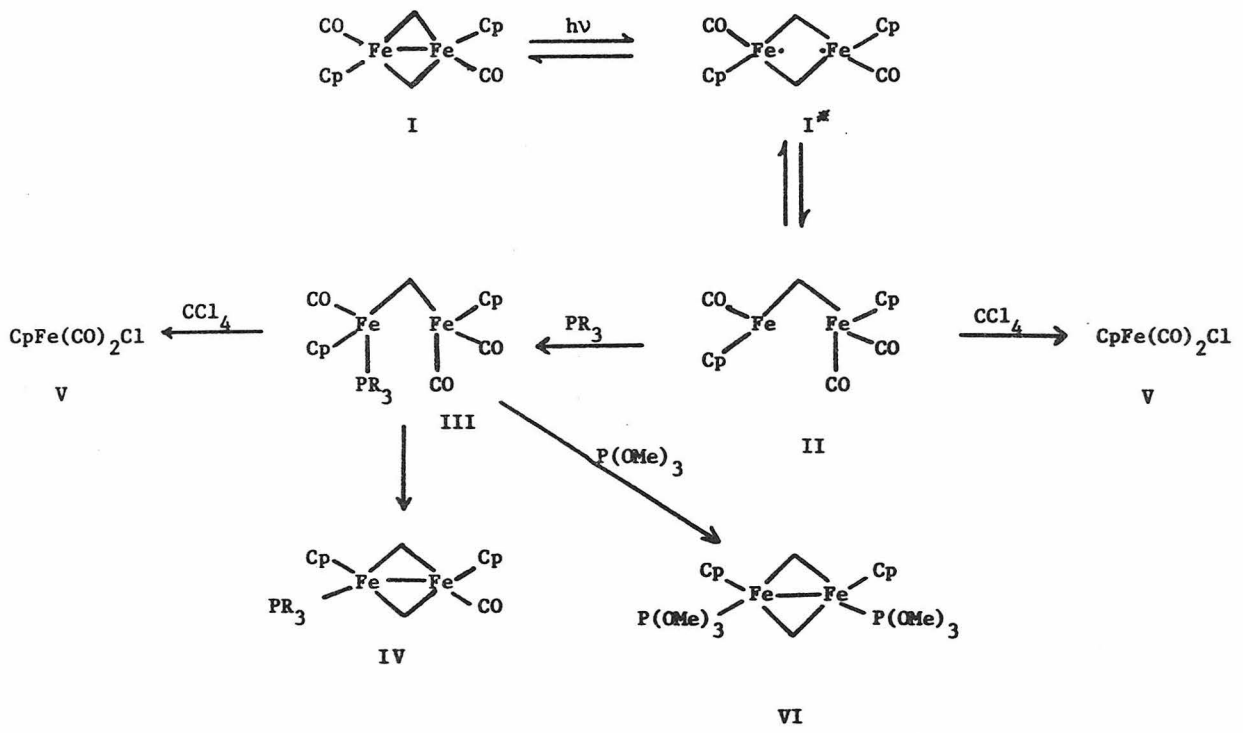
CO
Fe
Fe
Cp
CO
hν
I
I*
II
III
IV
V
VI
CCl4
PR3
P(OMe)3
CpFe(CO)2Cl

shown that photochemical phosphine substitution in $Mn_2(CO)_{10}$, a molecule with no carbonyl bridging groups, follows the pathway below (17).

$$Mn_2(CO)_{10} \xrightarrow{h\nu} 2Mn(CO)_5$$

$$Mn(CO)_5 + PR_3 \longrightarrow Mn(CO)_4PR_3 + CO$$

$$2Mn(CO)_4PR_3 \longrightarrow Mn_2(CO)_8(PR_3)_2$$

$$Mn(CO)_5 + Mn(CO)_4PR_3 \longrightarrow Mn_2(CO)_9PR_3$$

The primary photoprocess is homolytic cleavage of the Mn-Mn bond. This is followed by phosphine substitution for CO in the fragment molecule. Both mono- and disubstituted binuclear product complexes are observed. The lability of the 17-electron fragments is so great that the major product is the disubstituted dimer. If the photosubstitution of $Cp_2Fe_2(CO)_4$ occurred by the mechanism above, we might expect to see some disubstituted product, $Cp_2Fe_2(CO)_2(PR_3)_2$. Instead, near quantitative conversion to the monosubstituted complex occurs with PPh_3 and $P(OiPr)_3$ which suggests that simple homolytic cleavage of the bridged Fe-Fe unit is not the initial photochemical step.

Note that the two bridging carbonyl groups keep the two halves of the dimer from separating. However, if the excited state, I*, did not distort we believe that the metal-metal bond would easily reform thereby making the lifetime of the excited state too short to undergo a reaction with PR_3. Thus, one of the Fe-C bridging bonds must break, giving intermediate II. In this molecule one of the Fe atoms is coordinately-unsaturated (16 electrons). This coordinately-unsaturated Fe can react with a phosphine to give III which we propose is the thermally unstable yellow intermediate.

The spectroscopic data on the yellow intermediate is consistent with structure III. The infrared band at 1720 cm^{-1} is appropriate for a molecule with a bridging CO ligand (18) and the absence of a $\sigma \rightarrow \sigma^*$ band in the electronic spectrum indicates that the Fe-Fe bond has been broken (19). Finally, note that in the absence of phosphine, III will not form. This explains why the yellow intermediate forms only when phosphine is present.

The photosubstitution is completed, we propose, by dissociation of CO from III, followed by reformation of the Fe-Fe bond. Complex III is apparently stable enough at -78° that these last steps take place only on warming to higher temperatures.

To form the disubstituted product $Cp_2Fe_2(CO)_2(P(OMe)_3)_2$, the pathway in Figure 3 is simply repeated starting with $Cp_2Fe_2(CO)_3P(OMe)_3$ (12). Unlike the other $Cp_2Fe_2(CO)_3(PR_3)$ complexes discussed above, we found that $Cp_2Fe_2(CO)_3(P(OMe)_3)$ will react photochemically with

the excess phosphite in solution. We noted qualitatively that the photoreaction of $P(OMe)_3$ with $Cp_2Fe_2(CO)_3P(OMe)_3$ is much faster than the reaction of $P(OMe)_3$ with $Cp_2Fe_2(CO)_4$ and we suspect it is for this reason that no monosubstituted dimer is found. However, this is not to say that $Cp_2Fe_2(CO)_3P(OMe)_3$ is more photoreactive than the other monosubstituted dimers. Rather, $P(OMe)_3$ is simply a more reactive entering group. For instance, $P(OiPr)_3$ will not react photochemically with $Cp_2Fe_2(CO)_3(P(OMe)_3)$. But, $P(OMe)_3$ will react with the other monosubstituted dimers:

$$Cp_2Fe_2(CO)_3(P(OiPr)_3) + 2P(OMe)_3 \xrightarrow[\lambda \geq 366\ nm]{h\nu}$$

$$Cp_2Fe_2(CO)_2(P(OMe)_3)_2 + P(OiPr)_3 + CO$$

Apparently, the larger phosphines such as PPh_3, $P(O\text{-}iC_3H_7)_3$, and $P(n\text{-}C_4H_9)_3$ will not substitute twice because the attack by these phosphines on the coordinately unsaturated iron atom in II is prevented by steric crowding with the phosphine already substituted and the two Cp rings. Apparently, $P(OMe)_3$ is small enough that the reaction is not inhibited the second time.

We believe that intermediate II is also involved in the cross-coupling and chlorine abstraction reactions and that it is not necessary to propose the formation of 17-electron fragments as

primary photoproducts in these reactions. This conclusion follows from the following experimental result. When CCl_4 was vacuum distilled into a THF solution of intermediate III at -78° and the solution warmed to room temperature in the dark, the product was $CpFe(CO)_2Cl$. CCl_4 is able to displace the phosphine and react with the intermediate to give the chlorine abstraction product. The important point is that CCl_4 can react with the CO bridged, non metal-metal bonded intermediate (either II or III) to give $CpFe(CO)_2Cl$, and therefore, it is not necessary to postulate 17-electron fragment intermediates as primary photoproducts just because the chlorine abstraction product forms. This result also explains why $CpFe(CO)_2Cl$ is the only product in the photolysis of $Cp_2Fe_2(CO)_4$ with equimolar amounts of CCl_4 and PR_3. We also point out that the product of the competition experiment, $CpFe(CO)_2Cl$, is not consistent with a 17-electron fragment intermediate. If formed, the 17-electron fragments would be labile (17) and should substitute phosphines rapidly; some $CpFe(CO)(PR_3)Cl$ should form. Finally, the inhibition of the reaction of $Cp_2Fe_2(CO)_4$ with $CHCl_3$ by CO is consistent with the bimolecular reaction proposed in Figure 3. CO will bond at the vacant coordination site thereby preventing attack of the chlorocarbon solvent.

The other reactions, which it might be argued show that 17-electron fragments are intermediates, can also be explained by the bimolecular mechanism. For example, the reaction of $Mn_2(CO)_{10}$

would involve attack of an $Mn(CO)_5$ fragment on intermediate III. Also, the spin trapping experiments of Lappert using nitrosodurene could proceed by nucleophilic attack of the spin trap on III (20).

Other pathways might exist for the photoreactions discussed above. For example, it is possible to have a photochemical M-CO dissociation mechanism where Φ depends on the concentration of the substituting ligand. Thus, it might be argued that the primary photoprocess is simply dissociation of CO from the dimer. We have ruled out this possibility because it cannot explain the yellow intermediate. The dimeric unit obtained after Fe-CO dissociation would be $Cp_2Fe_2(CO)_3$. Recall that the yellow intermediate forms only when a phosphine is present. Thus, $Cp_2Fe_2(CO)_3$ cannot be the intermediate because it would form whether a phosphine was present or not. Nor can this molecule be the precursor to the intermediate because addition of phosphine to $Cp_2Fe_2(CO)_3$ would simply yield the stable product $Cp_2Fe_2(CO)_3(PR_3)$. Yet, another pathway might involve the initial photochemical conversion of a h^5-Cp ligand (6-electron donor) to a h^4-Cp ligand (4-electron donor). This would create a vacant coordination site and a PR_3-capture reaction would be possible. Such a pathway is unlikely, we feel, because of the natures of the lowest energy electronic excited states which most certainly involve a weakening of the Fe-Fe bond.

References and Notes

1. B. F. G. Johnson, J. Lewis, and M. V. Twigg, J. Organomet. Chem. 67, C75 (1974).
2. D. R. Tyler, R. A. Levenson, and H. B. Gray, J. Am. Chem. Soc. in press.
3. M. S. Wrighton, Top. Curr. Chem. 65, 68 (1977).
4. (a) O. S. Mills, A. A. Hock, and G. Robinson, Abstract A, XVIIth Internat. Cong. Pure Appl. Chem., Munich, 143 (1959); (b) K. Farmery, M. Kilner, R. Greatrex, and N. W. Greenwood, J. Chem. Soc. (A), 2339 (1969).
5. D. R. Tyler and H. B. Gray, manuscript in preparation.
6. O. S. Mills, Acta Cryst. 11, 620 (1958).
7. D. R. Tyler, M. A. Schmidt, and H. B. Gray, manuscript in preparation.
8. R. J. Haines and A. L. Du Preez, Inorg. Chem. 8, 1459 (1969).
9. J. G. Calvert and J. N. Pitts, Photochemistry, John Wiley and Sons, Inc., New York (1966).
10. W. D. Bowman and J. N. Demas, J. Phys. Chem. 80, 2434 (1976).
11. E. E. Wegner and A. W. Adamson, J. Am. Chem. Soc. 88, 394 (1966).
12. Another pathway is possible. When trimethyl phosphite is added to a cold solution (-78° C) of $Cp_2Fe_2(CO)_4(P(OiPr)_3)$, III, and the solution allowed to warm to room temperature in the dark, the product is $Cp_2Fe_2(CO)_2(P(OMe)_3)_2$. Apparently,

$P(OMe)_3$ can react with the non-metal-metal bonded intermediates (either II or III) to give the disubstituted dimer without initial formation of $Cp_2Fe_2(CO)_3(P(OMe)_3)$.

13. Ethyl chloride (Eastman) was used because it is still a liquid at -78°. THF will also work. $Cp_2Fe_2(CO)_4$ will not abstract Cl atoms from ethyl chloride.

14. K. Noack, J. Inorg. Nucl. Chem. 25, 1383 (1963).

15. R. B. King, P. M. Treichel, and F. G. A. Stone, Chem. Ind. (London), 747 (1961).

16. D. C. Harris and Harry B. Gray, Inorg. Chem. 14, 1215 (1975).

17. D. L. Kidd and T. L. Brown, J. Am. Chem. Soc. 100, 4095 (1978).

18. P. Chini, Pure Applied Chem. 23, 489 (1970).

19. R. A. Levenson and H. B. Gray, J. Am. Chem. Soc. 97, 6042 (1975).

20. A. Hudson, M. F. Lappert, and B. K. Nicholson, J. Chem. Soc., Dalton Trans. 551 (1977).